nature chemistry

REVIEW ARTICLE

PUBLISHED ONLINE: 21 MARCH 2014 | DOI: 10.1038/NCHEM.1889

The power of ion mobility-mass spectrometry for structural characterization and the study of conformational dynamics

Francesco Lanucara[1,2], Stephen W. Holman[1,2], Christopher J. Gray[2] and Claire E. Eyers[1,2]*

Mass spectrometry is a vital tool for molecular characterization, and the allied technique of ion mobility is enhancing many areas of (bio)chemical analysis. Strong synergy arises between these two techniques because of their ability to ascertain complementary information about gas-phase ions. Ion mobility separates ions (from small molecules up to megadalton protein complexes) based on their differential mobility through a buffer gas. Ion mobility-mass spectrometry (IM-MS) can thus act as a tool to separate complex mixtures, to resolve ions that may be indistinguishable by mass spectrometry alone, or to determine structural information (for example rotationally averaged cross-sectional area), complementary to more traditional structural approaches. Finally, IM-MS can be used to gain insights into the conformational dynamics of a system, offering a unique means of characterizing flexibility and folding mechanisms. This Review critically describes how IM-MS has been used to enhance various areas of chemical and biophysical analysis.

Ion mobility spectrometry (IMS) is an analytical technique that separates gas-phase ions based on their size and shape, analogous to electrophoresis in the condensed phase. The technique has long been used for the detection of illegal or dangerous substances, for example explosives at border crossings, and to garner evidence for the illegal use of chemical agents[1]. Mass spectrometry (MS) is also used in the analysis of gas-phase ions, permitting determination of their mass-to-charge (m/z) ratios. Therefore, the two techniques can be used to ascertain complementary information about analytes. The coupling of the two strategies, although first described in 1962[2], has only recently become relatively commonplace, primarily owing to commercialization of the necessary instrumentation. The past 10 or so years have seen an explosion in research using IM-MS, as demonstrated by a rapid increase in the annual number of peer-reviewed publications (Fig. 1), where the benefits of combining both analytical strategies have been exploited.

Instrumentation for ion mobility spectrometry

Primarily, three IMS techniques are used in IM-MS: drift-time ion mobility spectrometry (DTIMS), travelling-wave ion mobility spectrometry (TWIMS) and field-asymmetric ion mobility spectrometry (FAIMS) (Fig. 2, Table 1); these are described in detail below.

Drift-time ion mobility spectrometry. DTIMS is the oldest and conceptually simplest form of ion mobility (Fig. 2a). Ions are introduced into a drift tube. The application of a static uniform electric field (5–100 V) then propels these ions in the direction of the applied field. The tube is filled with a drift gas, typically helium. The time taken for an ion to drift through the tube is related to its rotationally averaged cross-sectional area—that is, the area covered by a particle, or more simply its collision cross-section (CCS), Ω. Compact structures travel faster than more elongated (extended) ions, owing to fewer interactions with the gas. The recorded drift time of an ion allows calculation of Ω, according to the Mason–Schamp equation[3]:

$$\Omega = \frac{3ze}{16N}\left(\frac{2\pi}{\mu k_B T}\right)^{1/2}\frac{1}{K_0}$$

where K_0 is the reduced mobility (measured mobility at standard temperature and pressure), z is the charge state of the ion, e is the elementary charge, N is the number density of the drift gas, μ is the reduced mass of the ion–neutral drift gas pair, k_B is the Boltzmann constant and T is the gas temperature. The proportional relationship between Ω and K_0 is only true at or below the 'low-field limit', where the ratio between electric field strength and buffer gas density is small, ≤2 townsend (2×10^{-17} V cm^2) (ref. 4). Determination of the CCS (which gives an indication of an ion's size and shape) provides structural information that is characteristic for each compound, and can be compared with data acquired using other structural techniques such as X-ray crystallography and nuclear magnetic resonance (NMR) spectroscopy. The level and quality of structural information obtainable using IMS compared with traditional techniques will be discussed below. DTIMS has advantages over other ion mobility devices because of its high resolving power ($R > 100\ \Omega/\Delta\Omega$), meaning that an ion with Ω of 1,000 Å^2 can theoretically be separated from an ion with ±10 Å^2 difference in Ω. DTIMS can, however, suffer from low duty cycle — that is, the percentage of ions detected relative to those generated by the ionization source — on devices where the ions are pulsed into the drift cell, or where entry or exit of ions into the drift cell occurs through extremely small apertures. Limitations in duty cycle have been overcome in newer-generation DTIMS instruments by incorporation of some form of ion-trapping funnel before the drift cell, which can accumulate ions while a previous pulse is being mobility-separated[5,6].

[1]Protein Function Group, Department of Biochemistry, Institute of Integrative Biology, University of Liverpool, Crown Street, Liverpool L69 7ZB, UK, [2]Michael Barber Centre for Mass Spectrometry, Manchester Institute of Biotechnology, School of Chemistry, University of Manchester, 131 Princess Street, Manchester M1 7DN, UK.
*e-mail: CEyers@Liverpool.ac.uk

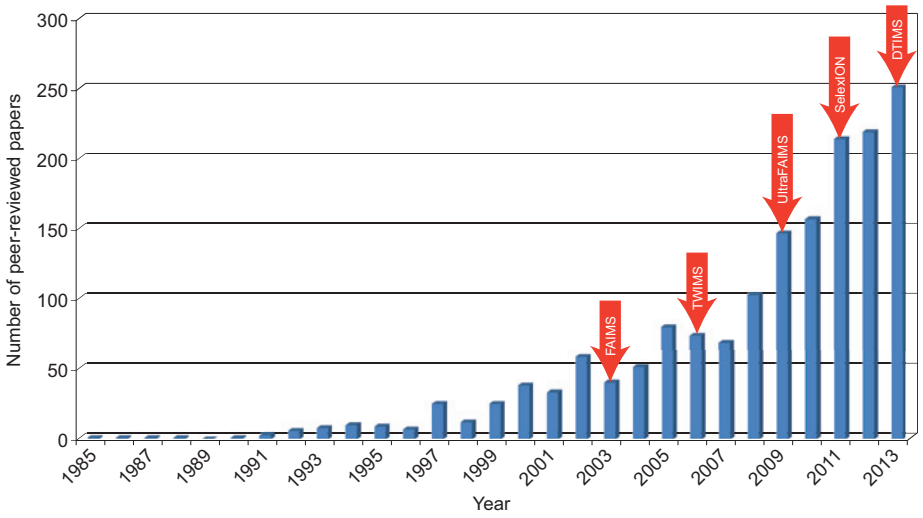

Figure 1 | Number of peer-reviewed papers published annually (to end of 2013) combining ion mobility and mass spectrometry. Data generated using Web of Science, SCI-expanded between 1985 and 2013, search terms 'ion mobility' and 'mass spectrometry'. Arrows indicate the years that various commercial ion mobility devices were made available. UltraFAIMS (Owlstone) and SelexION (ABSciex) are variants of the FAIMS device described below.

Travelling-wave ion mobility spectrometry. A TWIMS device comprises a series of ring electrodes called a stacked ring ion guide (SRIG), to which a travelling voltage wave is applied[7]. Radio-frequency voltages of opposite phases are applied to adjacent electrodes (Fig. 2b). These voltages radially confine the ions, while application of a transient direct current (DC) voltage to each electrode in succession from one end of the device to the other propels the ions axially. The DC voltage pulse applied to each electrode in turn creates the 'travelling wave' upon which ions 'surf' and traverse the mobility cell. By altering the speed and magnitude of the travelling voltage wave, mobility separation of ions can be achieved. Higher-mobility ions are 'carried' by the wave, whereas ions of lower mobility 'roll over' the wave, thus taking longer to move through the gas-filled mobility cell. Complex mixture separation can be achieved by sending several travelling waves through the device in quick succession.

The TWIMS device is operated below the low-field limit and, following calibration, determination of CCS is therefore possible[8–11]. Calibration of the drift time through the TWIMS cell under defined conditions (gas type/pressure, travelling wave speed or height, and so on) is necessary as the direct relationship between Ω and K_0 is no longer applicable, owing to the constantly changing electric field. Optimal drift-time calibration requires measurement of analytes of similar physical and chemical features with known CCS, to ensure that conditions are suitable for both calibrant and analyte. Although relatively simple to perform, the calibration does increase analysis time. The ability to use TWIMS with and without CCS calibration means that the technique has found application as both a separation device and a structural tool.

Field-asymmetric ion mobility spectrometry. FAIMS devices are constructed of two electrodes, across which an electric field is established (Fig. 2c)[12]. Ions are introduced into the device perpendicular to the electric field and collinearly to the drift gas. Two voltages are used to achieve separation: the dispersion voltage and the compensation voltage. The dispersion voltage is an alternating asymmetric waveform, where the value of the positive voltage is greater than that of the negative. The negative voltage is applied for a longer time, however, resulting in an equal (voltage × time) product for each part of the waveform (Fig. 2c). This waveform exploits the fact that under conditions of high electric field (>5,000 V s^{-1}), as generated by the positive voltage period, the mobility of ions can be different from that under the low electric field (<200 V s^{-1}) provided by the negative voltage period. This electric-field-dependent mobility means that ions drift radially as they traverse the electrodes (Fig. 2c). Ultimately, dispersion of the ions in this manner would lead to contact with the electrodes and neutralization. Therefore, to refocus ions through the electrodes, a compensation voltage is applied. For a given compensation voltage, only ions of specific mobility will be repelled from the electrodes, whereas other ions will continue along their path and be neutralized. Manipulation of the compensation voltage can therefore be used to selectively permit ions of interest through the electrodes while removing ions of differing mobility. The FAIMS device thus operates as a mobility filter and typically finds application as an orthogonal separation technique to liquid chromatography, separating ions based on different physicochemical properties, before MS analysis, enabling increased selectivity and peak capacity[13].

The main limitation of FAIMS is that CCS cannot be determined because its operating electric field strength causes it to exceed the low-field limit (Table 1); this prohibits the correlation of drift time with structural features, as the mobility of an analyte is not directly related to its structure, explaining why FAIMS devices are primarily used to filter out unwanted interferences or to separate analytes of interest. Although the resolving power of FAIMS separation is traditionally poor ($R<20$), the preferential inclusion of light gases (He or H_2) in the carrier gas (N_2), in which the ions are more mobile, has been demonstrated to increase resolution significantly, with resolving powers of up to 500 being reported[14–16].

Like FAIMS, the differential mobility analyser (DMA) is a spatial mobility device rather than a time-based separation device such as DTIMS or TWIMS. Unlike FAIMS, however, DMAs do not invoke alternating high and low electric fields to induce analyte separation, instead using the combined force of a high-flow-rate sheath gas and a superimposed electric field applied perpendicular to the gas flow in order to filter ions[17,18]. DMA instruments have historically been used in the area of aerosol science for the analysis of particles over ~10 nm in diameter and have not achieved the same popularity as FAIMS devices[17,19]. Newer-generation DMA instrumentation with higher resolving power ($R>50$) may yet encourage growth in this area[20].

Summary. Although the IMS devices discussed will all separate ions according to differences in their mobility through a buffer gas, only the time-based mobility devices (DTIMS, TWIMS) can be used to determine information about cross-sectional area, either with or without the requirement for drift-time calibration if there is a need

to define CCS in Å^2. In contrast, FAIMS (and DMA) devices function preferentially as filtration devices, much as quadrupoles can be used in MS analysis. Regardless of whether the utility of IMS separation is for analyte filtration and/or differentiation, or more targeted structural analysis, the key strength comes in combining this analytical feature with MS, because of the complementary information garnered. Examples of how IMS devices can be used either to improve the mass-spectrometry-based analysis of complex mixtures, or, in the case of DTIMS/TWIMS, to aid enhanced structural analysis and the study of conformational dynamics are described below.

Enhancing MS analysis of mixtures with IMS

The coupling of IMS to MS can significantly improve experimental analysis as defined by a range of criteria often used to benchmark such methods: selectivity, speed and limit of detection. The improvement gained for each is considered below.

Selectivity. The complementary mode of separation introduced by the coupling of any type of IMS device to MS analyses can lead to improved selectivity and thus an enhanced ability to interrogate mixtures. Creese and Cooper exploited the separation capability of FAIMS to resolve isomeric glycopeptides differing only by the site of glycosylation[21]. The isomers co-eluted when using liquid chromatography, making glycosite localization extremely difficult. Because these species were of the same *m/z* value they were co-isolated before MS/MS analysis, thus generating a chimeric mass spectrum of product ions composed of fragments from both isomers. Incorporating FAIMS allowed separation of these glycopeptides based on their different mobilities, and thus selective acquisition of MS/MS data for each of the isomers, enabling definitive characterization. Many similar experiments have been conducted to resolve and characterize complex mixtures of small molecules[22]. Analytes may also have similar mobilities and thus drift time, meaning that they comigrate during IMS, although this can often be overcome by altering the applied voltages (timing or amplitude), changing the drift gas or adding volatile (often chiral) dopants, such as 2-butanol[23,24]. Detailed studies have shown that the change in selectivity induced by such dopants is obtained through differential formation of ion–molecule clusters[25,26].

Addition of shift reagents, as used in NMR spectroscopy, is another strategy that can improve the separation of ions of similar mobility in their native forms[27–29]. Selective complex formation of only one of the compounds with the shift reagent changes their mobility and aids separation. One particularly effective use of this approach was reported by Howdle and co-workers, who used a pharmaceutical excipient, polyethylene glycol (PEG), already present in the sample as the shift reagent[27]. Inclusion of PEG changed the mobility of the target drug, lamivudine, so that it occupied an interference-free region of the spectrum and could be analysed in isolation.

The separation capabilities of IMS have also demonstrated particular utility in MS analyses where chromatographic separation either has not been or cannot be used, providing a crucial additional analytical dimension. For example, MS imaging experiments, where analytes are ionized directly from a complex matrix such as a tissue section, are notably enhanced by incorporation of IMS (ref. 30). Stauber and co-workers used TWIMS in a matrix-assisted laser desorption/ionization (MALDI)-MS imaging experiment to separate

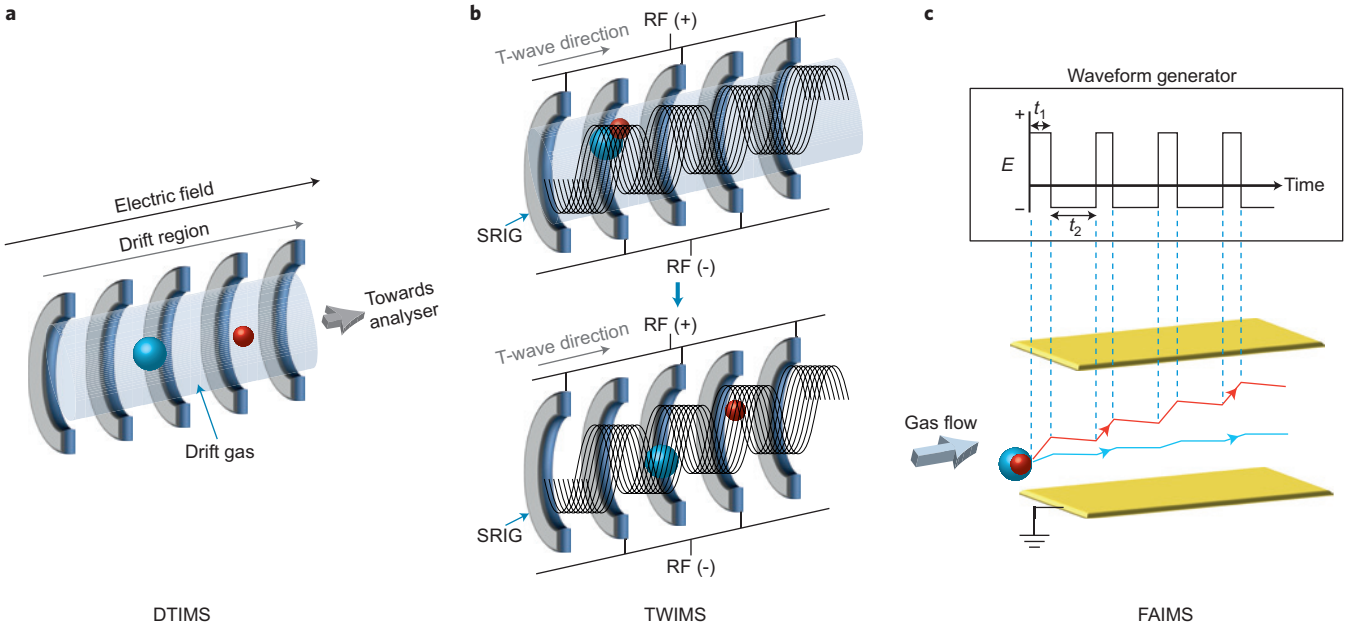

Figure 2 | Schematic diagrams of the main types of ion mobility device. Small ions are in red, large ions are in blue. **a**, DTIMS, used for direct calculation of an ion's CCS (Ω) by means of the Mason–Schamp equation. Separation is achieved by passing the ions through a drift gas along the axis of an applied electric field. The flight of a small ion (red) is retarded to a lesser degree than a large ion (blue), owing to fewer interactions with the drift gas. The time taken to traverse the device (the drift time) is correspondingly shorter. **b**, TWIMS, used for both CCS calculation (after calibration of the drift time with ions of similar Ω and charge state), and differential separation of ions in a complex mixture. Application of a travelling voltage wave (T-wave) to a series of electrically connected ring electrodes (stacked ring ion guide; SRIG) pushes ions through the device. Separation is achieved because, for a given wave speed and magnitude, higher-mobility ions (red) will be carried forward by the wave, whereas lower-mobility species (blue) will roll over the wave, thus taking longer to exit the device. RF, radio-frequency. **c**, FAIMS, used primarily for differential separation of ions in a complex mixture. Introduction of ions into an alternating asymmetric electric field (E) causes them to drift towards the two electrodes at different rates. Time at positive voltage (t_1) is shorter than the time at negative voltage (t_2), although an equal (voltage × time) product for each part of the waveform is maintained. Application of a DC voltage, termed the compensation voltage (CV), repels the ions and refocuses their flight through the device. Different analytes require different CVs to prevent collision with the electrodes. In this case, the analyte with the smaller CCS (red) drifts quickly towards the electrode and requires a high CV to refocus it through the device. The analyte with the larger CCS (blue) is less affected by the RF voltage and travels towards the electrode more slowly, and thus requires a lower CV to correct its trajectory.

Table 1 | Comparison of the three main types of IMS.

	DTIMS	TWIMS	FAIMS
Advantages	Rotationally averaged collisional cross-section (CCS; Ω), that is, 'shape' can be measured (Å^2) Can be used to separate species of very similar mobility; high resolving power (>100 as defined by $\Omega/\Delta\Omega$ measured at FWHM)[157]	Rotationally averaged CCS can be determined Can be used for mobility separation of product ions generated either by collision-induced dissociation or by electron-transfer dissociation	High resolving power (≤ ~100 as defined by $\Omega/\Delta\Omega$ at FWHM)[14] Relatively straightforward to transfer the ion mobility device between different mass spectrometers
Disadvantages	The geometric configuration of current commercial DTIMS-MS instruments means that they can only be used to separate analytes immediately post-ionization Gating-type instruments are susceptible to ion losses when transferred from atmospheric pressure during ionization to the reduced pressure required for analysis	CCS determination requires calibration of the drift time through the TWIMS cell, ideally using a calibrant of similar physical and chemical properties Relatively low resolving power (≤~45 as defined by $\Omega/\Delta\Omega$ at FWHM)[152] Ion heating can occur as ions are injected into the TWIMS cell which may affect gas-phase conformation. Unless carefully controlled, the process of measurement may therefore perturb analyte structure	CCS cannot be determined The geometric configuration of a FAIMS-MS instrument means that it can only be used to separate analytes immediately post-ionization The percentage of ions detected relative to those generated following ionization (that is, the duty cycle) is relatively low when operated under conditions where the CV is ramped (CV scanning mode), reducing sensitivity

CV: compensation voltage; FWHM: full width at half maximum.

isobaric ions (those of the same nominal m/z value)[31]. Whereas analysis of these ions in the absence of IMS produced a composite image of two species, meaning that distinct localization could not be ascertained, incorporation of IMS allowed acquisition of separate spatial distributions for each individual compound. A similar study recorded the spatial distribution of the cytotoxic agent vinblastine following its administration to rats. Although this analysis initially suffered from matrix interference at the same m/z value as the target compound, the additional selectivity afforded by TWIMS enabled vinblastine distribution to be accurately determined[32].

Another area where the additional separation provided by IMS has proved beneficial is non-targeted discovery proteomics. Shliaha and co-workers used liquid chromatography (LC)-TWIMS-MS to analyse a tryptic digest of an *Escherichia coli* whole-cell lysate, and demonstrated a ~60% increase in the number of identifications at both the peptide and protein levels compared with LC-MS alone[33]. A similar study comparing the same analytical strategies reported an even greater increase in the number of identifications, with both peptide and protein assignments rising because of the complementary separation mechanism and additional peak capacity afforded by the TWIMS device[34].

Speed. In many areas of (bio)chemistry and medical science, high-throughput sample analysis is critical. IMS is a technology that can expedite analysis and thus is likely to play an increasing role in numerous fields where rapid analysis is required, for example drug screening. IMS typically works on the millisecond timescale, faster than chromatography (typically on the scale of seconds), and could potentially be used to increase the speed of analysis while retaining the necessary separation. Parson and co-workers separated isomeric glucuronide metabolites of propranolol over 15 times faster using FAIMS than had been achieved using high-performance liquid chromatography (HPLC)[35]. Many other examples exist of IMS being used to improve the rate of pharmaceutical discovery and/or screening by obviating (or significantly reducing) the need for chromatographic separation before MS. For example, application of TWIMS significantly increased the rate at which biological samples could be screened for the presence of natural products as potential leads for therapeutic drugs[36]. TWIMS has also been used in metabonomics to provide additional online separation, reducing the duration of the upstream liquid chromatography method and thus improving throughput[37].

Limit of detection. The limit of detection by MS is much lower than for most other analytical techniques, with LC-MS routinely detecting low attomole amounts of analyte even in complex mixtures[38,39]. The addition of IMS to the analytical workflow can lower limits of detection further by removing background interference. The group of Thibault demonstrated a greater than 10-fold improvement in the detection limits of peptides in complex mixtures when FAIMS was incorporated into their LC-MS platform[40]. The improved limits of detection and increased power of separation doubled the number of peptide[40] and phosphopeptide[41] identifications from unpurified cellular extracts. Likewise, Ibrahim and co-workers used a set of model isomeric modified peptides to demonstrate that DTIMS can overcome the necessity to fragment peptides for discovering the site of covalent modification, using instead the mobility of each isomer for characterization[42]. By incorporating DTIMS for ions of known behaviour, determined using authentic standards, these researchers circumvented the need for tandem MS and reported an order-of-magnitude improvement in detection limits.

The qualitative and quantitative analysis of therapeutics in complex biological matrices can also be improved using IMS; for example, TWIMS aided the detection of peptide drugs by enabling the identification of low-abundance metabolites following the removal of background chemical 'noise' in a complex mixture[43]. Furthermore, FAIMS has been used to remove a matrix component in plasma that prevented a LC-MS assay for the drug dianicline from passing acceptance criteria for good laboratory practice[44]. The additional separation provided by incorporation of FAIMS significantly decreased the limit of detection, thus making the analytical approach more effective for assaying the drug. The same technology was used by Guddat and co-workers, who developed methodologies for the detection of performance-enhancing steroids and their metabolites in urine samples taken from athletes, reducing the detection limits in some cases to subpicogram per millilitre (pg ml^{-1}) quantities[45]. Improvements in detectability open up the future possibility of identifying a wide range of substances in biological fluids at significantly lower levels (and for longer periods post-dosage), with important implications for monitoring healthcare and the screening of drugs of abuse.

IMS for enhanced structural analysis of (bio)molecules

Although all modes of ion mobility spectrometry will separate analytes on the basis of their conformation, application of DTIMS or TWIMS can further be used to determine CCS. Unlike other biophysical techniques used to characterize analyte structure, IM-MS can be used to ascertain structural information using only small amounts of sample (nanogram quantities). Moreover, as the ions of interest can be selectively isolated from complex samples, material of much lower purity can be used than is typically needed to structurally characterize compounds using X-ray crystallography or NMR spectroscopy (Table 2)[46]. Furthermore, by using IM-MS to determine changes in mobility and thus conformation and CCS, properties such as conformational dynamics[47–52], folding and unfolding intermediates[52–54], ligand-induced conformational changes[55,56], aggregation intermediates[57,58] and quaternary structures (topology) can be determined[59–60].

Determination of ion collision cross-sections. Analyte structure is determined from experimentally derived, rotationally averaged temperature-dependent CCS values, which reflect the conformation and shape adopted by the ions in the gas phase under defined experimental conditions[61]. Experimental CCS can be compared with theoretical CCS values generated by molecular dynamic (MD) simulations, often using X-ray and NMR structures as input for the calculations[62–65]. Computational algorithms have been developed for this purpose, although choosing the right algorithm is extremely important for correct interpretation of the experimental IM-MS data. When dealing with large proteins and protein complexes, the complexity brought about by the range of molecular shapes and dimensions that arise pose serious limitations to the applicability of such algorithms, either because of their inability to deal with particular kinds of intra- and intermolecular interactions, or because of the extremely demanding computational costs.

The most common models used to calculate CCS are projection approximation (PA)[66], exact hard-sphere scattering (EHSS)[67] and the trajectory method (TM)[68], all of which determine the CCS using helium as the buffer gas. The PA method is relatively computationally inexpensive, calculating CCS as an average of geometric projection areas of all the possible orientations of the molecule. It does not, however, take into account long-range interactions or many of the features arising because of scattering between the ions and the drift gas. Owing to its inability to factor in multiple collisions, this method usually underestimates CCS for ions over 2 kDa and is therefore primarily used for predicting CCS of small molecules. The EHSS method takes account of the scattering and the collisions with the drift gas but ignores long-range interactions between gas and ions. In contrast, the trajectory method is generally considered more reliable, particularly for large biomolecules, as it takes into account long-range interactions between the drift gas and the analyte ion, as well as collision effects[69]. An important limitation of the trajectory method, however, is the time required to perform calculations, particularly for very large molecules; for such analytes, the EHSS method is therefore often a good compromise.

Recently, the projection superposition approximation (PSA) method was introduced by Bleiholder and co-workers[70–73]. Like projection approximation, PSA computes molecular shapes as a projection approximation, but with an extra feature of superposition of atomic potentials and inclusion of a shape factor. This approach is of particular value considering that long-range, attractive van der Waals interactions between ions and buffer gas are proportional to the analyte's molecular weight and the atom density, and are therefore a function of the molecular shape. An algorithm that is capable of taking into account these size and shape effects, concomitantly lowering computational demands, is therefore particularly beneficial. The PSA method was shown to outperform EHSS following tests on three sets of molecules chosen to represent different sizes and shapes, providing results in very good agreement with the trajectory method, but with a 100–1,000-fold reduction in computational time[70].

IM-MS as a stand-alone technique for structural studies. Most of the detailed structural interpretation of CCS values generated through IM-MS relies on the availability of total or partial structures (either crystalline or solution phase) as input for the prediction of comparative CCS values. But independent of the availability of X-ray- or NMR-derived structures, gas-phase IM-MS is a powerful tool for the interrogation of dynamic systems without the perturbation brought about by solvation effects, counter-ions and the presence of other chemical species that may bind and alter analyte conformation. This offers a unique medium to explore intrinsic physicochemical properties, and measurement of ionic mobilities (and the consequent determination of the associated CCS values) permits understanding of the conformational landscapes that different ionic species can populate. Furthermore, as discussed below, the possibility of extracting ions of interest from near-native solutions as 'naked' species allows one to explore the effect of sequential binding of solvent molecules on structure, thus enabling insights into the role of hydration on conformational dynamics. Partial or total unfolding of a protein is often reflected in the observation of higher charge states due to the exposure of a greater number of protonation sites, and has an immediate effect on their ionic mobilities[74]. Similarly, ligand binding or protein post-translational modification often induces conformational changes that can be evaluated using IM-MS without necessarily having to rely on the availability of calculated CCS values (that is, prior detailed structural determination), and such measurements have also been used to explore temperature-dependent conformational dynamics[75]. Indeed, one might argue that IM-MS is a unique analytical tool for (bio)molecules unsuited to conventional approaches.

Importantly, unlike many other biophysical techniques that provide an averaged structure, IMS can be used to interrogate dynamic heterogeneity, placing IM-MS in a privileged position over both crystallography and NMR spectroscopy (Table 2). The ability to monitor dynamics allows snapshots of short-lived folding intermediates and conformational transitions to be obtained[47,48]. Identification of transient conformations is becoming more commonplace as the techniques develop: recent work from Shvartsburg and colleagues has demonstrated the additional utility of different drift gases, notably hydrogen-rich gas mixtures, for enhancing the separation of dynamic protein conformers by FAIMS[76]. The five-fold improvement in resolution achieved under these conditions enabled distinction of ~15 conformations of ubiquitin, where previously only a handful of conformers had been distinguishable. This strategy will undoubtedly prove invaluable for future investigation into protein conformation. For biopolymers such as proteins and protein complexes, investigation of both conformation and dynamics furthers our understanding of the intramolecular and intermolecular interactions that control the folding and the conformational landscapes that biomolecules can adopt *in vacuo*. A comparison of the results obtained in the gas phase with data obtained for the same system in solution can improve our understanding of the role played by solvent molecules, counter-ions and other chemical entities in driving the formation of thermodynamically stable structures (see below).

The additional dimension of separation offered by ion mobility in IM-MS also means that the resolution of isobaric and isomeric molecular species is feasible. This has enormous potential in the case of polymeric systems where subunits can generate different types of multimeric assembly that would not be distinguishable by virtue of their m/z value alone. As illustrated by examples below, IM-MS has been successfully used to explore oligomerization processes of polypeptides such as β-amyloid, whose aggregation is linked to the aetiology of neurodegenerative diseases[77,78].

Small molecules (<500 Da). IM-MS analysis of small molecules, especially naturally occurring metabolites and molecules derived

Table 2 | Some advantages and disadvantages of commonly applied analytical techniques for determining structural information about analytes[158,159].

	IM-MS	MS^n *	NMR spectroscopy	X-ray crystallography	Circular dichroism
Phase of analyte during analysis	Gas	Gas	Liquid (or solid)	Solid	Liquid (gas/solid)
Advantages	Very sensitive Can analyse mixtures Fairly rapid for simple structures, with the most time-consuming parts being molecular dynamics simulations Under carefully controlled ionization and acquisition conditions, can be used to determine structure from native conditions Can determine stoichiometry of complexes Measures 3D structure in dynamic motion	Very sensitive Can analyse mixtures Fairly rapid, aided by mass spectra search engines and spectral databases Can determine stoichiometry of complexes Products of electron-mediated dissociation can be used to infer 3D structure	Non-destructive Can be very rapid when analysing smaller molecules (<500 Da) As most biologically relevant compounds are found in aqueous media, the ability to perform solution-state NMR spectroscopy means that structure can be analysed under native-like conditions May allow stereochemical information, bond angles and distances to be elucidated Conventional solution-state NMR spectroscopy can measure 3D structure in dynamic motion	Non-destructive Can directly determine structural information at the atomic level May allow stereochemical information, bond lengths and angles to be elucidated	Non-destructive Can measure exchanging structures (>picoseconds) Rapid direct diagnostic test for certain structural features, for example relative helicity Can determine native structural features Allows determination of stereochemistry
Disadvantages	Analyte must be able to be ionized Relies on molecular dynamics simulations to indirectly determine precise structural information from CCS values; simulations become more challenging as molecules become larger Destructive	Analyte must be able to be ionized Difficult to ascertain detailed 3D structure information directly from mass spectra Destructive	Difficult to analyse mixtures of products; samples often have to be purified and concentrated, which may affect the structure of biological samples Analysis of spectra becomes difficult for larger molecules	Requires purified and crystallized material; may be time-consuming or impossible to generate crystals Analyte may be damaged by the X-rays	Cannot be used for mixtures. Requires relatively concentrated (~0.5 mg ml^{-1}) purified samples Gives no specific structural information at the atomic level

*MS^n refers to multistage MS/MS experiments designed to record product ion spectra where *n* is the number of stages of mass analysis[160].

following the metabolism of exogenous compounds, is gaining impetus. Metabolites are usually present in biological samples at levels far too low for structural characterization using NMR spectroscopy. LC-MS/MS, although having a limit of detection suitable for metabolite analysis, will often be unable to discriminate between isomeric species even after multiple rounds (*n*) of MS analysis (MS^n)[65]. This is especially true for aromatic hydroxylated metabolites. Dear and co-workers overcame this limitation by applying TWIMS-MS and molecular dynamics simulations to the analysis of ondansetron and its metabolites, thereby allowing the 6-, 7- and 8-(OH) regioisomers to be discerned, even though they generated identical product ion mass spectra (Fig. 3)[64]. Regioisomers of glucuronidated metabolites have also been distinguished and identified using TWIMS-MS[79]. Determining the CCS of product ions generated by collisional dissociation, in addition to the precursor ion from which they are derived, may also be useful as molecular dynamics simulations are more accurate for molecules with fewer degrees of freedom[80]. Such studies may also allow stereochemical information to be harnessed that would otherwise be difficult to determine from the precursor ion alone. For example, in a recent study, Both *et al.* used drift time measurements to differentiate the stereochemistry of monosaccharide product ions generated after collision-induced dissociation (CID) of glycopeptides and free di-, tri- and pentasaccharides, suggesting that IM-MS^n may be useful for glycan sequencing[81]. Clemmer and colleagues have also used a new IMS/ion-trap hybrid instrument to determine the ion mobility distributions (and thus conformation) of select precursor ions by monitoring for specific CID products[82], a strategy which could feasibly be extended to other types of product ions, such as those arising following electron transfer dissociation (ETD). IM-MS has also been shown to be capable of resolving diastereoisomers indistinguishable by HPLC, MS and NMR spectroscopy, and that were unsuitable for X-ray diffraction owing to the formation of polycrystalline solids[80].

Peptides. When combined with molecular dynamics simulations, IM-MS is a powerful tool to determine the secondary structure of peptides in the gas phase. In particular, studying peptide folding *in vacuo* is likely to be more physiologically relevant for polypeptides integral to a cell membrane, as the cell membrane interior and a vacuum both possess a low dielectric constant ($\varepsilon = 1$)[83]. Factors that influence the *in vacuo* formation of particular peptide secondary structure features (α-helices, β-sheets or globules) have been extensively studied by IMS[84–88]. IM-MS revealed that the *N*-terminally

acetylated peptide $[Lys\text{-}Ala_{15} + H]^+$ has a CCS consistent with a globular structure solvating the charge, an important driving force in peptide secondary structure folding *in vacuo*[84,86]. But relocation of lysine (Lys) to the *C*-terminus (generating *N*-terminally acetylated $[Ala_{15}Lys + H]^+$) seems to allow short-range solvation, and induction of an α-helical structure, stable to over 400 °C (ref. 84). Structural changes induced by the adduction of metal ions (cationization) to peptides have also been studied by IM-MS, revealing new information on the CCS of cationized versus protonated peptide ions. Also, and arguably potentially of greater interest, analogous studies have determined how conformation changes induced by metal-ion adduction can influence protein–ligand interactions[89–92].

IM-MS has also proved extremely useful in advancing our understanding of gas-phase peptide dissociation[93]. Studies on product ion conformations after CID of peptides have revealed that both linear and cyclic product ions are formed regardless of the energy deposited[94]. Subsequent ring opening of the resultant macrocycles at different positions leads to scrambling of the original linear peptide sequence, complicating sequence determination by tandem MS[95,96]. Furthermore, conformations adopted by gas-phase radical cationic products can now be more readily investigated with the development of a new commercial IM-MS instrument capable of performing ETD (ref. 97).

Large biomolecules. Early IM-MS studies of biologically relevant polymers focused on drift-time measurements of isolated small proteins (enabling CCS calculation), and were mainly used to improve understanding of the relationship between solution-phase and gas-phase conformations. Such structures had already been explored by measuring charge state distribution by electrospray ionization mass spectrometry (ESI-MS)[74], as lower charge states are generally believed to be more representative of the folded, compact conformations adopted by a protein in solution. But care should be taken in assuming that a reduced charge state always corresponds to a native structure (see below). Indeed, depending on the contribution of hydrophobic, ionic and hydrogen bond interactions, the three-dimensional structure might evolve in very specific ways upon desolvation. Therefore any general relationship between low charge state and compactness is hard to define *a priori*[74].

Proteins and protein complexes under native conditions

The possibility of generating gas-phase ions from solutions of controlled ionic strength and buffered pH enables interrogation of complex systems under near-physiological conditions. This is extremely valuable if structural properties are to be related to biological activity because features of the solution-phase conformation may sometimes be preserved[98–102]. ESI of proteins and protein assemblies generates several species with different charge states. Generally, more compact structures have a reduced number of exposed protonation sites, thus limiting the maximum charge on the corresponding gas-phase ions. IM-MS analyses of ions of reduced charge states are therefore optimal, as they are more likely to represent the biologically relevant, native folded species. But protein complexes containing a central cavity have been observed to collapse during IM-MS, yielding ions of low charge state with more compact structures, and thus smaller CCS values, than their native-like conformation[103].

A key concept in the IM-MS analysis of proteins and protein complexes from native conditions is the ability to transfer intact species from solution into the gas phase without inducing major conformational changes upon the loss of solvating molecules, as occurs during ESI (ref. 100). For a structural analysis to be meaningful, it is important to ensure that the structure being analysed resembles that of its native, functional state. Water molecules play a key role in controlling the stability of protein (and protein complex) conformations in solution, mainly by inducing hydrophobic regions to orient themselves towards the core of the structure and thus minimize contact with the aqueous solvent[104]. It has therefore been suggested that removal of these solvent molecules might induce important conformational changes leading to non-native ('inside-out') structures[69,105]. Considerable effort has been devoted to understanding the relationship between solution and gas-phase conformation both theoretically and experimentally, and much of the currently accepted theory in this area has been generated by IM-MS measurements[106–109].

Investigations into the role of hydration in controlling the stability and dynamics of protein conformations in the gas phase have provided significant insight into the many factors governing the folding and unfolding of gaseous protein ions[110–115]. Of particular relevance

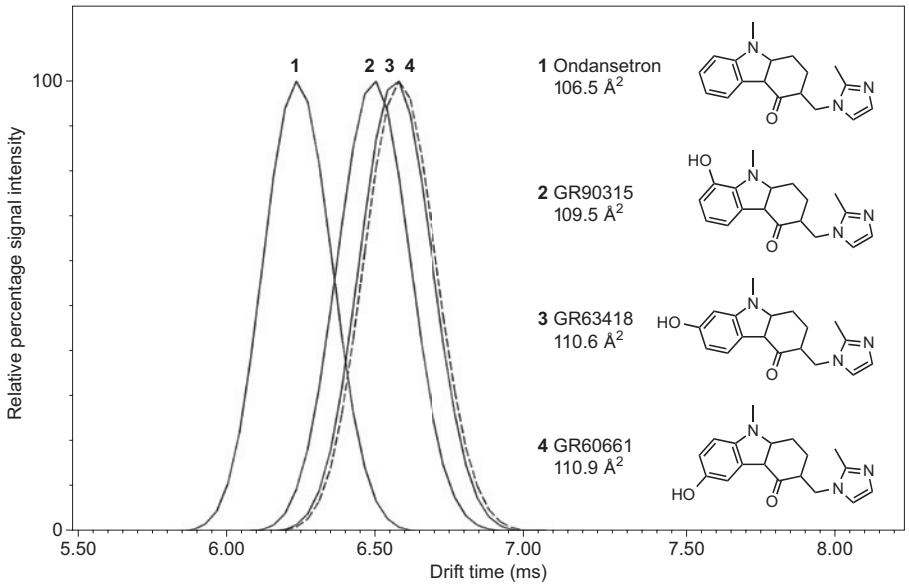

Figure 3 | Arrival-time distributions (ATDs) as determined by TWIMS, and structures of the parent drug ondansetron (1) and its isomeric metabolites. The metabolites **2** to **4** are GR90315 (8-hydroxy), GR63418 (7-hydroxy) and GR60661 (6-hydroxy), respectively. Metabolite **2** can clearly be discriminated from metabolites **3** and **4** by their respective ATDs following ion mobility separation, discrimination which would be impossible by mass spectrometry alone. ATD for **4** is differentiated from ATD for **3** by means of a dashed line. The experimentally determined collision cross-section values are reported in Å^2. Reproduced with permission from ref. 64, © 2010 Wiley.

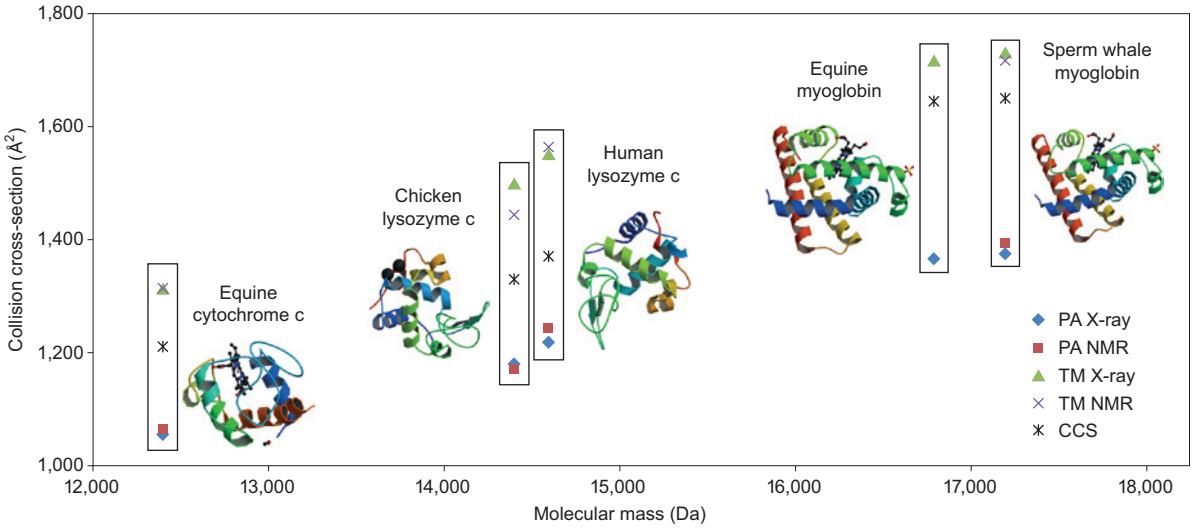

Figure 4 | Comparison of experimentally estimated CCS of five protein standards. CCS values (in Å^2), calculated using either the projection approximation (PA) or the trajectory method (TM) from available X-ray and NMR structures of the same proteins, are plotted for each of the proteins together with the CCS as determined by TWIMS. The crystallographic structures obtained from the PDB files in the RSCD Protein Data Bank (www.rcsb.org/pdb) are depicted. Chicken lysozyme c PDB IDs: 1DPX (X-ray), 1GXX (NMR); human lysozyme c PDB IDs: 2NWD (X-ray); 1IY3 (NMR); sperm whale myoglobin PDB IDs: 1VXG (X-ray), 1MYF (NMR); equine myoglobin PDB ID: 1WLA (X-ray); equine cytochrome c PDB IDs: 1HRC (X-ray); 1LC1 (NMR). Figure adapted with permission from ref. 46, © 2008 Wiley.

are studies of gas-phase hydration of folded and unfolded protein ions by DTIMS-MS in which ESI-generated cytochrome c ions were allowed to react with water in the drift tube of the ion mobility device. The arrival time distributions (ATDs) of fully desolvated ions were then compared with those of ions carrying an increasing number of solvent molecules[112]. Using this approach, Fye and co-workers demonstrated that an unfolded charge state ($z = 7$) characterized by two peaks in the fully desolvated state shifted towards the more compact folded conformation (with earlier arrival time) upon hydration. This pioneering study suggested that the addition of water molecules to unfolded gas-phase protein ions promotes refolding towards more compact, native-like structures. Similar studies have been reported by Rodriguez-Cruz and colleagues using (smaller) biological peptides such as gramicidin S, outlining the competition between charge solvation with water and internal 'self-solvation' by hydrogen bonds and their influence on gas-phase and solution-phase structures[110]. More recently, Gao and co-workers described the effect of hydration in the competition between salt bridges and charge solvation for isolated, protonated basic amino acids (arginine and lysine), showing how hydration of the gas-phase ions balances the competition between the two types of interactions, permitting formation of otherwise disfavoured salt bridges[115]. Such studies have advanced our understanding of the mechanisms of ESI and how this process can contribute to preserving or disrupting the original solution-phase structure[113].

Although IM-MS determined CCS values for lower charge states are generally in good agreement with data calculated for the same species based on X-ray crystallography or NMR spectroscopy data, gas-phase CCS values are typically slightly lower than those calculated for solid-phase crystal structures[69]. As recently reported for a collection of theoretical and experimental CCS values of proteins of different molecular weight, the discrepancy between the two sets of data tends to increase with the size of the protein[69]. Considering the fraction of crystal volume occupied by solvent molecules, this variation can be explained by invoking a partial collapse of the gas-phase protein ions upon desolvation[116]. DMA-MS studies have revealed a difference as large as 40% between the gas-phase CCS and the X-ray structure of the GroEL tetradecamer, suggesting substantial compaction of the native structure *in vacuo* and/or expansion on crystallization[117]. Despite this noticeable difference, the authors were still able to demonstrate that the tetradecameric complex maintains its native topology upon desolvation.

Figure 4 compares CCS values measured by TWIMS for the lowest charge state of five proteins (believed to be representative of the native conformations) with values calculated from solid-phase (X-ray crystallography) and solution-phase (NMR spectroscopy) studies using the projection approximation and trajectory theoretical methods described above[46]. The general observation of higher values derived from the trajectory method than those calculated using projection approximation is probably because the latter does not consider interactions of the ions with the buffer gas, meaning that for convex structures the CCS will be underestimated[66]. The experimentally determined CCS values are lower than the trajectory method values but higher than the projection approximation values for all five proteins. This is probably because gas-phase protein ions can adopt conformations that are more compact than those observed in the solid state, owing to partial collapse of the charged residues as a consequence of solvent removal[69,118]. A detailed description of the structural evolution of a globular protein during and after ESI has been presented by Breuker and McLafferty, who described how a gaseous environment can potentially induce important structural changes[118]. As well as the need to consider both covalent and non-covalent interactions that stabilize protein structures in solution, it seems that the time during which ions are allowed to relax in the gas phase before analysis is paramount in dictating whether the original conformation is preserved or a new, more stable gaseous conformation arises. IM-MS-derived structural data should therefore be interpreted with the caveat that desolvation can introduce changes in the overall gas-phase ion structure, and the degree of change will depend on both the experimental conditions and the analyte itself.

It is clear that the relationship between gas-phase and solution- and solid-phase conformations is not easily addressed, mainly because the changes which an ion undergoes upon transfer to the gas phase are largely dependent on the relative roles played by electrostatic and hydrophobic interactions in dictating the native structure. Nonetheless, IM-MS measurements of CCS of biologically interesting species, such as proteins and protein assemblies, are invaluable as they readily enable investigation of conformation dynamics and folding/unfolding equilibria that are not easily

accessible by solid-phase or solution-phase strategies. IM-MS therefore plays an important role in unravelling structural features. A recent example includes a study that used a 3D ion-trap/IM/quadrupole-time of flight (Q-ToF) instrument to monitor the effect of charge reduction on the conformation of gas-phase cytochrome c ions[119]. Protein ions of high charge state were selected to undergo proton transfer reactions in the ion trap, and the resulting CCS values compared with those of the same charge states extracted from the solution by ESI. The two values were similar, suggesting that initially unfolded, highly charged species can be induced to refold to their original compact states through charge reduction. These elegant experiments, which could only be achieved by coupling an ion trap with IM-MS, permitted researchers to follow conformational transitions and demonstrate how Coulombic-induced unfolding might be reversed. Analogous experiments followed the temporal evolution of ESI-generated conformations of several charge states of cytochrome c over a timescale ranging from 10 ms to 10 s, demonstrating that initially folded conformations can relax into new minima on the conformational potential energy surface by temporarily populating unfolded intermediates[120]. A similar study on the evolution of the native and a partially unfolded state of ubiquitin using DTIMS was also recently reported by Wyttenbach and Bowers[121]. The compact state was found to survive for up to 100 ms *in vacuo*, whereas the 'A state', extracted from an acidic solution expected to induce partial unfolding, showed a faster (≤100 ms) decay to conformational intermediates, which then further refolded to new compact species. Electron paramagnetic resonance spectroscopy in combination with TWIMS-MS has also revealed information about the conformational dynamics and molecular recognition processes which contribute to the functioning of the NarJ chaperone protein when bound to its substrate NarG[122]. ESI-IM-MS measurements of the unbound and bound chaperone under native solution conditions clearly demonstrated that substrate binding was dependent on recognition and selection of a single conformer.

Despite recent advances, structural investigation of membrane proteins remains particularly challenging, owing to the difficulty in solubilizing these species in buffers compatible with ESI while preserving their native structure. Much work has been done to demonstrate that native protein conformations can be maintained under the relatively harsh conditions required to release hydrophobic proteins from stabilizing detergent micelles during ESI, although this process needs to be carefully controlled[123,124]. As an alternative to detergents as solubilizing agents that may unduly influence protein structure, Leney *et al.* recently described an amphipathic polymer for solubilizing two bacterial, β-barrel-functional outer-membrane proteins in a detergent-free solution before IM-MS analysis[125]. Once in the gas phase, the proteins were released from their complexes with the polymer by voltage-induced activation in the source and transfer regions of the mass spectrometer, and their conformational properties were studied by TWIMS. Both proteins retained their native structures based on comparison with theoretically predicted CCS, highlighting the potential of IM-MS for the examination of membrane proteins. Such strategies will undoubtedly be of great importance, considering the interest that these, and other, membrane proteins have garnered as therapeutic targets.

The analysis of pathways leading to the formation of non-covalent, insoluble protein aggregates, such as amyloid fibrils, which are associated *in vivo* with the onset of pathological states including Parkinson's and Alzheimer's disease, has been revolutionized by IM-MS (ref. 126). Of particular relevance are contributions by the Bowers group, including a fundamental study characterizing the mechanism of amyloid-β protein oligomerization and generation of toxic amyloid fibrils[77], and investigations into the effects of spermine binding on α-synuclein protein conformation leading to protein compaction, a likely precursor for α-synuclein aggregation and the onset of Parkinson's disease[78]. Measurement of drift times (and calculation of experimental CCS values) for different protein assemblies and prediction of model structures for the amyloid-β aggregates using the projection approximation model allowed specific pathways to be defined for the observed self-assembling processes, showing the potential of IM-MS as a complementary, and yet independent, structural tool for the investigation of these challenging systems. In addition to permitting structural characterization of the intermediate, oligomeric species in aggregate formation[57,77,127], these studies used ion mobility to deconvolute isobaric peaks in the mass spectrum, originating from combinations of different numbers and charge states of homo-oligomers that coalesce to the same m/z value[128]. Analogous studies using DTIMS[129,130] or TWIMS[131] have also been used to investigate the binding mode of inhibitors (small molecules, peptide mimetics and peptides) on formation of toxic β-amyloid aggregates, providing evidence for the mechanism of action of effective therapeutic agents for the potential treatment of Alzheimer's disease.

The field of IM-MS analysis of large protein assemblies was pioneered by Robinson and colleagues, and represents an exciting area of application for this powerful technique. For example, analysis of the trp RNA binding attenuation protein (TRAP)[60] provided compelling evidence that many features of protein assemblies, including quaternary structure, can be preserved in the absence of solvent molecules. Indeed, this was the first IM-MS study to succeed in showing that a large multimeric protein assembly (relative molecular mass of 90 kDa) could be transferred from aqueous solution to the gas phase while maintaining its quaternary topology[60]. The researchers made use of TWIMS coupled to a modified ToF mass spectrometer to measure the CCS of four charge states (19^+–22^+) of the 11-mer complex, demonstrating that the lowest charge state exhibited the largest CCS, with a value in close agreement to that estimated for a ring structure determined by X-ray crystallography. Further details of the identity of the conformers underlying this ionic population were provided by thorough molecular dynamic simulations using the EHSS method, showing how the experimentally determined CCS for the 19^+ charge state comprised the native ring structure as well as partial ring and buckled ring conformers. IM-MS studies also revealed how binding of a 53-base-pair strand of RNA to the TRAP complex had a stabilizing effect on the gas-phase conformation.

Another fertile research area is virus structure and assembly, with the Heck group[59] reporting IM-MS analysis of hepatitis B virus (HBV) capsids as large as 4 MDa. These virus particles are known to form two icosahedral capsids of different sizes depending on the number of dimers: T3 with 90 or T4 with 120 dimers. TWIMS-MS analysis identified two distinct conformations for each of the virus capsids, generating CCS values that were found to be in close agreement with the radii obtained for the same structures analysed by electron microscopy.

The study of membrane-embedded molecular machines represents a challenge from a structural determination point of view and has been revolutionized by IM-MS in conjunction with other MS-based techniques. Other biophysical techniques have been able to analyse subunits of these large protein machineries, generating a wealth of informative data but failing to report any structural characterization of intact complexes. The first report on the gas-phase structure of an intact adenosine triphosphatase (ATPase)/synthase machinery appeared in 2011 using an IM-MS instrument specifically modified for transmission of high-mass complexes[132,133]. The recorded mass spectra revealed the subunit stoichiometries for the two complexes, and ion mobility studies of the transmembrane proteins within the complex demonstrated conformational heterogeneity of subunit I (in ICL_{12}), but not subunit CL_{12} (as determined by a broader ATD of ICL_{12}) (Fig. 5). It was only by using this IM-MS-derived structural data that a mechanism of function of this proton channel could be proposed[133].

Other large molecules

Many large compounds have been studied by IMS, including deoxyribonucleic acids (DNA)[134], macrocycles[135] and synthetic polymers[136]. These large molecules often retain their solution-phase structure in the gas phase for (up to) milliseconds[137].

The gas-phase conformations adopted by different DNA secondary structures, including hairpins, pseudoknots and cruciforms (Holliday junction), have been studied using both IM-MS and molecular dynamics (Fig. 6). At lower charge density, all of these secondary structures are stable over the typical millisecond timescale of ion mobility analysis. Where both pseudoknots and hairpins can be formed, pseudoknots are found to be favoured because of the formation of extra Watson–Crick pairs between the initial secondary structure formed (usually a hairpin) and another single-stranded region. At higher charge density these structures become elongated as Watson–Crick pairs are broken. Interestingly, the cruciform that was extensively studied formed a B-helix in the solution phase, although this same analyte was found to exist as both a B-helix and an A-helix when desolvated, demonstrating that IM-MS can be used as a tool to study structures adopted in a solvent-free environment[134]. G-quadruplex formation, of particular importance in understanding the mechanism of cellular ageing and transformation, has also been monitored by IM-MS. In solution, these structures are known to form stacked planar rings where the plane is formed from four guanosine residues stabilized by atypical Hoogsteen hydrogen bonds and cations between the planes[138]. These structures are retained upon vaporization, as confirmed by IM-MS. Analysis of tandem repeats of the telomeric region, where G-quadruplexes are often observed, allowed distinction and determination of G-quadruplex isomers[139]. Using IM-MS, the intermediates in the assembly of these G-quadruplexes could be characterized and it was only by using such a strategy that it could be demonstrated that the final kinetically stable tetramers form an equilibrium state of DNA monomers, dimers and trimers, upon addition of ammonium cations[140].

Polymer chemistry is also beginning to use IM-MS as a structure elucidation tool, with polar homopolymers often exhibiting sharper ATDs than proteins[136]. Early experiments were performed on thermally stable PEG ions coordinating a single alkali metal cation[141,142]. For Li^+ and Na^+, PEG seemed to coil around the cation, forming a similar structure to a classical crown ether to solvate charge. Precise structures differed depending on the size of the PEG oligomers and the number of oxygen atoms that were capable of coordinating to the metal cation; whereas Li^+ and Na^+ coordinated with seven and eight oxygen atoms respectively, Cs^+ coordinated with 10–11 oxygen atoms, exhibiting a different conformation[141]. Investigations into other polymeric systems have also indicated that, like polypeptides, they become more extended as charge is increased, owing to Coulombic repulsion[136,143]. Recently, structures of intermediates and mechanisms of gas-phase thermal polymerization of styrene have been analysed by IM-MS, highlighting the possible application of this technology for directly monitoring gas-phase reactions and polymerization chemistry[144].

Synthetic systems including metal-ring host–guest complexes, rotaxanes, catenanes, macrocyclic porphyrin-like systems and synthetic baskets such as resorcinarenes represent an exciting branch of chemistry, owing to their potential applications in biosensing, drug delivery, catalysis and materials engineering. In many cases, the interaction between host and guest is controlled by fine structural differences, such as *cis–trans* isomerism. In-depth characterization is therefore challenging, especially when classical biophysical methodologies are not applicable. The coupling of ion mobility to MS offers a unique strategy to address the structural features of these systems with evident advantages over other techniques: different chemical entities can be resolved by virtue of their m/z values before measuring their gas-phase conformations, without the need for highly pure, concentrated sample solutions and with high speed of analysis. Recent studies have highlighted the importance of IM-MS to resolve very similar structures: *cis–trans* cyclometallated cages[145] and rigid coordination-based rectangular, triangular and prismatic platinum-complexes[146] were separated using DTIMS-MS; regio- and stereoisomeric pairs of multi-ruthenated porphyrins[147] and entire libraries of supramolecular assemblies using TWIMS[148]. In many instances, prediction of candidate structures by molecular modelling was used to help to corroborate these results.

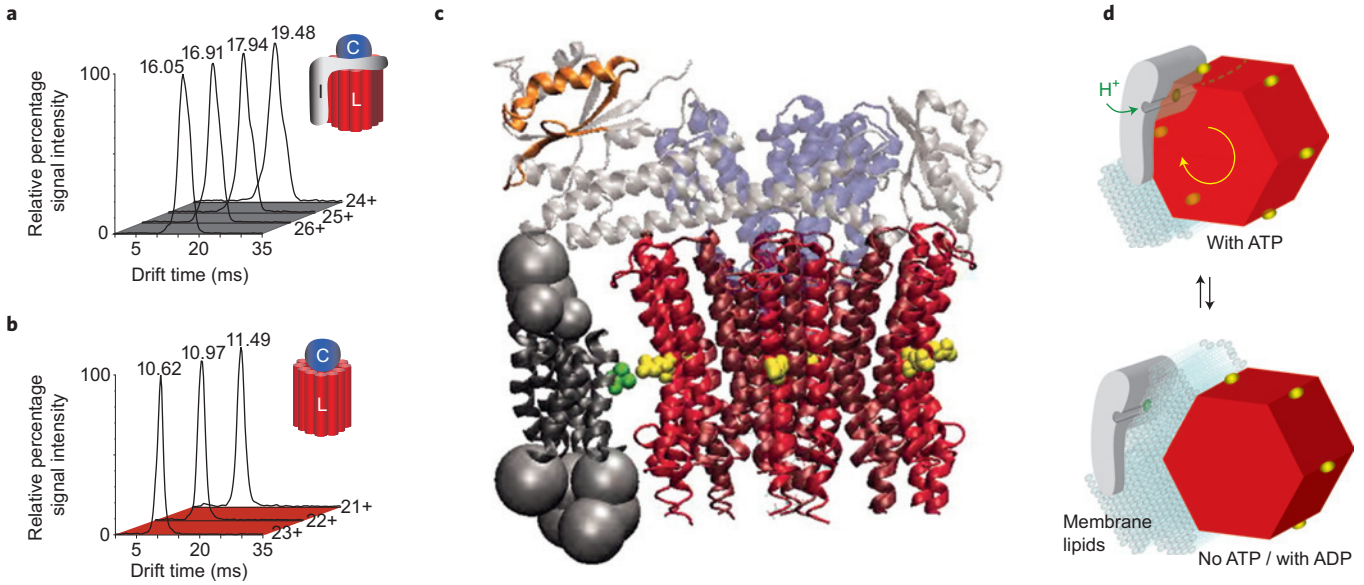

Figure 5 | Conformational heterogeneity and dissociation of subunit I from ICL12 implies a mechanism for closing the H+ channel. a,**b**, Arrival-time distributions (ATDs) are shown for ICL_{12} (**a**) and CL_{12} (**b**) complexes. The broader ATDs observed for selected charge states of the intact ICL_{12} complex are indicative of multiple conformations of the subunit I. **c**, Coarse-grained and atomic model of complex ICL_{12} based on spatial restraints as defined by IMS. The flexible subunit I is shown in grey, with the nucleotide binding region highlighted in orange. **d**, Proposed mechanism for the closure of the proton channel upon lateral movements of the subunit I (view from the top). Mass spectrometry identifies loss of the subunit I under low [ATP] and low [H^+] concentrations; the gap left between subunit L and the rest of the complex can then be filled with membrane lipids. Adapted with permission from ref. 133, © 2011 AAAS.

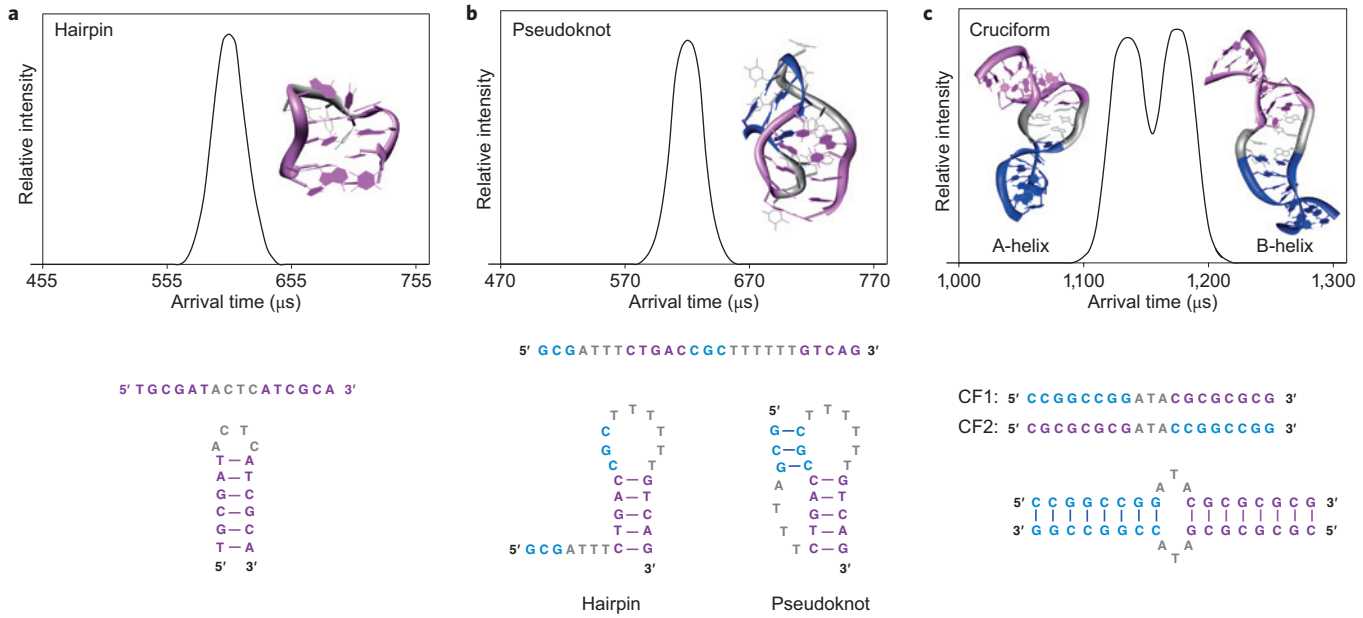

Figure 6 | Polynucleotide structures as determined using a combination of molecular dynamic simulations and experimentally determined ATDs. Depicted (top) are the ATDs and structures as predicted using molecular dynamics (MD), together with the polynucleotide sequence(s) and expected conformations (bottom). **a**, 5′-TGCGATACTCATCGCA-3′ adopts a hairpin secondary structure where the nucleotide backbone 'loops' back to form a series of Watson–Crick pairs. **b**, 5′-GCGATTTCTGACCGCTTTTTTGTCAG-3′ could adopt one of two potential conformations, forming either a hairpin structure, or a pseudoknot where two loops are formed and held in place by Watson–Crick pairs to the adjacent nucleotide sequence. Molecular dynamics and IM-MS measurements both indicate the presence of a single structure corresponding to the pseudoknot. **c**, The DNA strands CF1 (5′-CCGGCCGGATACGCGCGCG-3′) and CF2 (5′-CGCGCGCGATACCGGCCGG-3′) together form two IM-resolvable structures, which molecular dynamics shows to be cruciform secondary structures adopting both A and B helical conformations. Adapted with permission from ref. 134, © 2009 ACS.

Conclusions and future perspectives

The broad-ranging utility of IM-MS instrumentation by scientists in academia, process chemistry, pharmaceutical science and biotechnology is spurring rapid developments in instrument design and use, with next-generation instrumentation demonstrating improvements in versatility, resolution and limits of detection compared with earlier models[149,150]. Continuous advances in both ion optics[151] and the mobility devices themselves[152–155], which increase ion transmission and instrument resolving power, are significantly improving IMS capability, enabling studies of larger analytes at submicromolar concentrations. For example, the inclusion of high-pressure electrodynamic ion funnels (originally developed by Smith and colleagues)[156] either side of the drift cell has improved IMS resolution without negatively influencing sensitivity, because mobility separation can be performed at higher pressures[151]. The more recent development of a cyclical ion drift tube with ion-trapping capabilities to enhance ion current has further improved the resolving power of ion mobility separation ($R > 1{,}000$), although the sensitivity of such measurements is currently poor[155]. Further developments in ion transmission will undoubtedly lead to better performance. Future commercial availability of different combinations of hybrid ion mobility and MS instrumentation with improved specifications and greater versatility can only enhance the already broad utility of this powerful analytical strategy.

Traditionally, MS, which operates on the microsecond timescale, has been combined with chromatographic separation (either liquid or gas) operating in the region of seconds to minutes, for the analysis of mixtures. Ion mobility separation typically operates on the millisecond timescale, and consequently can be nested between chromatographic separation and MS analysis. Thus, the benefits of IMS for improved analysis of mixtures can be obtained without detriment to the already established complementarity of chromatography and MS. We expect that gas chromatography/liquid chromatography (GC/LC)-IM-MS will become standard for optimal analytical capability in many situations. But considerable improvements in ion mobility resolution will be required for it to 'outperform' recent developments in ultra-high-performance liquid chromatography, and its benefits for high-throughput analyte separation lie in its ability to separate ions by different physicochemical properties.

A great strength of IM-MS is the ability to characterize and compare dynamic changes in analyte structure. This has previously been extremely difficult to do for most biological samples. At present IM-MS studies often require 'validation' by other strategies, in part owing to natural scepticism towards new (or rather unfamiliar) techniques. But the field is now approaching sufficient maturity that it should be possible for IM-MS-generated structural information, acquired under carefully controlled conditions, to stand on its own merits. Indeed, structures inferred from X-ray crystallography should ideally be used to complement, rather than purely validate, the gas-phase conformational information generated by IM-MS. IMS is limited in that it is not capable of providing detailed atomic-level structural information. This is counterbalanced, however, by its utility in studying conformational dynamics of rapidly evolving systems.

Like MS before it, we believe that IM-MS is rapidly becoming an invaluable tool for wide-ranging chemical analysis, with different modes of IMS used for specific experimental requirements: that is, discrimination of compounds in mixtures versus determination of CCS values. That ion mobility can be used both for analyte separation and structural investigation of a wide range of sample types makes it an extremely powerful addition to the analytical 'toolbox' of all chemists and biochemists.

Received 19 March 2013; accepted 11 February 2014; published online 21 March 2014

References

1. D'Agostino, P. A. & Chenier, C. L. Desorption electrospray ionization mass spectrometric analysis of organophosphorus chemical warfare agents using ion mobility and tandem mass spectrometry. *Rapid Commun. Mass Spectrom.* **24,** 1617–1624 (2010).

2. McDaniel, E. W., Martin, D. W. & Barnes, W. S. Drift-tube mass spectrometer for studies of low-energy ion-molecule reactions. *Rev. Sci. Instrum.* **33,** 2–7 (1962).
3. Mason, E. A. & Schamp, H. W. Jr. Mobility of gaseous ions in weak electric fields. *Ann. Phys.* **4,** 233–270 (1958).
4. Creaser, C. S. *et al.* Ion mobility spectrometry: a review. Part 1. Structural analysis by mobility measurement. *Analyst* **129,** 984–994 (2004).
5. Wyttenbach, T., Kemper, P. R. & Bowers, M. T. Design of a new electrospray ion mobility mass spectrometer. *Int. J. Mass Spectrom.* **212,** 13–23 (2001).
6. Harvey, S. R., MacPhee, C. E. & Barran, P. E. Ion mobility mass spectrometry for peptide analysis. *Methods* **54,** 454–461 (2011).
7. Giles, K. *et al.* Applications of a travelling-wave based radio-frequency-only stacked ring ion guide. *Rapid Commun. Mass Spectrom.* **18,** 2401–2414 (2004).
8. Bush, M. F. *et al.* Collision cross sections of proteins and their complexes: a calibration framework and database for gas-phase structural biology. *Anal. Chem.* **82,** 9557–9565 (2010).
9. Campuzano, I. *et al.* Structural characterization of drug-like compounds by ion mobility mass spectrometry: Comparison of theoretical and experimentally derived nitrogen collision cross sections. *Anal. Chem.* **84,** 1026–1033 (2012).
10. Bush, M. F., Campuzano, I. D. & Robinson, C. V. Ion mobility mass spectrometry of peptide ions: Effects of drift gas and calibration strategies. *Anal. Chem.* **84,** 7124–7130 (2012).
11. Chawner, R. *et al.* QconCAT standard for calibration of ion mobility-mass spectrometry systems. *J. Proteome Res.* **11,** 5564–5572 (2012).
12. Purves, R. W. & Guevremont, R. Electrospray ionization high-field asymmetric waveform ion mobility spectrometry-mass spectrometry. *Anal. Chem.* **71,** 2346–2357 (1999).
13. Canterbury, J. D., Yi, X., Hoopman, M. R. & MacCoss, M. J. Assessing the dynamic range and peak capacity of nanoflow LC-FAIMS-MS on an ion trap mass spectrometer for proteomics. *Anal. Chem.* **80,** 6888–6897 (2008).
14. Shvartsburg, A. A., Danielson, W. F. & Smith, R. D. High-resolution differential ion mobility separations using helium-rich gases. *Anal. Chem.* **82,** 2456–2462 (2010).
15. Shvartsburg, A. A. & Smith, R. D. Accelerated high-resolution differential ion mobility separations using hydrogen. *Anal. Chem.* **83,** 9159–9166 (2011).
16. Shvartsburg, A. A. *et al.* High-definition differential ion mobility spectrometry with resolving power up to 500. *J. Am. Soc. Mass Spectrom.* **24,** 109–114 (2013).
17. Knutson, E. O. & Whitby, K. T. Aerosol classification by electric mobility: Apparatus, theory, and applications. *J. Aerosol Sci.* **6,** 443–451 (1975).
18. Pomareda, V., Lopez-Vidal, S., Calvo, D., Pardo, A. & Marco, S. A novel differential mobility analyzer as a VOC detector and multivariate techniques for identification and quantification. *Analyst* **138,** 3512–3521 (2013).
19. de la Mora, J. F., de Juan, L., Eichler, T. & Rosell, J. Differential mobility analysis of molecular ions and nanometer particles. *TRAC Trend. Anal. Chem.* **17,** 328–339 (1998).
20. Rus, J. *et al.* IMS-MS studies based on coupling a differential mobility analyzer (DMA) to commercial API-MS systems. *Int. J. Mass Spectrom.* **298,** 30–40 (2010).
21. Creese, A. J. & Cooper, H. J. Separation and identification of isomeric glycopeptides by high field asymmetric waveform ion mobility spectrometry. *Anal. Chem.* **84,** 2597–2601 (2012).
22. Varesio, E., Le Blanc, J. C. Y. & Hopfgartner, G. Real-time 2D separation by LC x differential ion mobility hyphenated to mass spectrometry. *Anal. Bioanal. Chem.* **402,** 2555–2564 (2012).
23. Howdle, M. D., Eckers, C., Laures, A. M-F. & Creaser, C. S. The effect of drift gas on the separation of active pharmaceutical ingredients and impurities by ion mobility-mass spectrometry. *Int. J. Mass Spectrom.* **298,** 72–77 (2010).
24. Fernández-Maestre, R., Wu, C. & Hill, H. H. Jr. Using a buffer gas modifier to change separation selectivity in ion mobility spectrometry. *Int. J. Mass Spectrom.* **298,** 2–9 (2010).
25. Fernández-Maestre, R., Wu, C. & Hill, H. H. Jr. Buffer gas modifiers effect resolution in ion mobility spectrometry through selective ion-molecule clustering reactions. *Rapid Commun. Mass Spectrom.* **26,** 2211–2223 (2012).
26. Holness, H. K., Jamal, A., Mebel, A. & Almirall, J. R. Separation mechanism of chiral impurities, ephedrine and pseudoephedrin, found in amphetamine-type substances using achiral modifiers in the gas phase. *Anal. Bioanal. Chem.* **404,** 2407–2416 (2012).
27. Howdle, M. D., Eckers, C., Laures, A. M-F. & Creaser, C. S. The use of shift reagents in ion mobility-mass spectrometry: Studies on the complexation of an active pharmaceutical ingredient with polyethylene glycol excipients. *J. Am. Soc. Mass Spectrom.* **20** (2009).
28. Hilderbrand, A. E., Myung, S. & Clemmer, D. E. Exploring crown ethers as shift reagents for ion mobility spectrometry. *Anal. Chem.* **78,** 6792–6800 (2006).
29. Bohrer, B. C. & Clemmer, D. E. Shift reagents for multidimensional ion mobility spectrometry-mass spectrometry analysis of complex peptide mixtures: evaluation of 18-Crown-6 Ether Complexes. *Anal. Chem.* **83,** 5377–5385 (2011).
30. Kiss, A. & Heeren, R. M. A. Size, weight and position: ion mobility spectrometry and imaging MS combined. *Anal. Bioanal. Chem.* **399,** 2623–2634 (2011).
31. Stauber, J. *et al.* On-tissue protein identification and imaging by MALDI-ion mobility mass spectrometry. *J. Am. Soc. Mass Spectrom.* **21,** 338–347 (2010).
32. Trim, P. J. *et al.* Matrix-assisted laser desorption/ionization-ion mobility separation-mass spectrometry imaging of vinblastine in whole body tissue sections. *Anal. Chem.* **80,** 8628–8634 (2008).
33. Shliaha, P. V., Bond, N. J., Gatto, L. & Lilley, K. S. Effects of travelling wave ion mobility separation on data independent acquisition in proteomics studies. *J. Proteome Res.* **12,** 2323–2339 (2013).
34. Rodriguez-Suarez, E. *et al.* An ion mobility assisted data independent LC-MS strategy for the analysis of complex biological samples. *Curr. Anal. Chem.* **9,** 199–211 (2013).
35. Parson, W. B. *et al.* Rapid analysis of isomeric exogenous metabolites by differential mobility spectrometry-mass spectrometry. *Rapid Commun. Mass Spectrom.* **25,** 3382–3386 (2011).
36. Esquenazi, E., Daly, M., Bahrainwala, T., Gerwick, W. H. & Dorrestein, P. C. Ion mobility mass spectrometry enables the efficient detection and identification of halogenated natural products from cyanobacteria with minimal sample preparation. *Bioorgan. Med. Chem.* **19,** 6639–6644 (2011).
37. Harry, E. L., Weston, D. J., Bristow, A. W. T., Wilson, I. D. & Creaser, C. S. An approach to enhancing coverage of the urinary metabonome using liquid chromatography-ion mobility-mass spectrometry. *J. Chromatogr. B* **871,** 357–361 (2008).
38. Picotti, P., Bodenmiller, B., Mueller, L. N., Domon, B. & Aebersold, R. Full dynamic range proteome analysis of *S. cerevisiae* by targeted proteomics. *Cell* **138,** 795–806 (2009).
39. Brownridge, P. *et al.* Global absolute quantification of a proteome: Challenges in the deployment of a QconCAT strategy. *Proteomics* **2011,** 2957–2970 (2011).
40. Saba, J., Bonneil, E., Pomiès, C., Eng, K. & Thibault, P. Enhanced sensitivity in proteomics experiments using FAIMS coupled with a hybrid linear ion trap/orbitrap mass spectrometer. *J. Proteome Res.* **8,** 3355–3366 (2009).
41. Bridon, G., Bonneil, E., Muratore-Schroeder, Caron-Lizotte, O. & Thibault, P. Improvement of phosphoproteomic analysis using FAIMS and decision tree fragmentation. Application to the insulin signaling pathway in *Drosophila melanogaster* S2 cells. *J. Proteome Res.* **11,** 927–940 (2012).
42. Ibrahim, Y. M., Shvartsburg, A. A., Smith, R. D. & Belov, M. E. Ultrasensitive identification of localization variants of modified peptides using ion mobility spectrometry. *Anal. Chem.* **83,** 5617–5623 (2011).
43. Cuyckens, F. *et al.* Identifying metabolite ions of peptide drugs in the presence of an *in vivo* matrix background. *Bioanalysis* **4,** 595–604 (2012).
44. Blackburn, M. A. *et al.* Identification and subsequent removal of an interference by FAIMS in the bioanalysis of dianicline in animal plasma. *Bioanalysis* **3,** 2119–2127 (2011).
45. Guddat, S., Thevis, M., Kapron, J., Thomas, A. & Schänzer, W. Application of FAIMS to anabolic androgenic steroids in sport drug testing. *Drug Testing Anal.* **1,** 545–553 (2009).
46. Scarff, C. A., Thalassinos, K., Hilton, G. R. & Scrivens, J. H. Travelling wave ion mobility mass spectrometry studies of protein structure: Biological significance and comparison with X-ray crystallography and nuclear magnetic resonance spectroscopy measurements. *Rapid Commun. Mass Spectrom.* **22,** 3297–3304 (2008).
47. Gidden, J., Bushnell, J. E. & Bowers, M. T. Gas-phase conformations and folding energetics of oligonucleotides: dTG^- and dGT^-. *J. Am. Chem. Soc.* **123,** 5610–5611 (2001).
48. Gidden, J. & Bowers, M. T. Gas-phase conformational and energetic properties of deprotonated dinucleotides. *Eur. Phys. J. D* **20,** 409–419 (2002).
49. Wyttenbach, T., Grabenauer, M., Thalassinos, K., Scrivens, J. H. & Bowers, M. T. The effect of calcium ions and peptide ligands on the relative stabilities of the calmodulin dumbbell and compact structures. *J. Phys. Chem. B* **114,** 437–447 (2010).
50. Jenner, M. *et al.* Detection of a protein conformational equilibrium by electrospray ionisation-ion mobility-mass spectrometry. *Angew. Chem. Int. Ed.* **50,** 8291–8294 (2011).
51. Bereszczak, J. Z. *et al.* Structure, stability and dynamics of norovirus P domain derived protein complexes studied by native mass spectrometry. *J. Struct. Biol.* **177,** 273–282 (2012).
52. Shi, H., Pierson, N. A., Valentine, S. J. & Clemmer, D. E. Conformation types of ubiquitin $[M+8H]^{8+}$ ions from water:methanol solutions: Evidence for the N and A states in aqueous solution. *J. Phys. Chem. B* **116,** 3344–3352 (2012).
53. Smith, D. P., Giles, K., Bateman, R. H., Radford, S. E. & Ashcroft, A. E. Monitoring copopulated conformational states during protein folding events using electrospray ionization-ion mobility spectrometry-mass spectrometry. *J. Am. Soc. Mass Spectrom.* **18,** 2180–2190 (2007).
54. Nabuchi, Y., Hirose, K. & Takayama, M. Ion mobility and collision-induced dissociation analysis of carbonic anhydrase 2. *Anal. Chem.* **82,** 8890–8896 (2010).
55. Hyung, S-J., Robinson, C. V. & Ruotolo, B. T. Gas-phase unfolding and disassembly reveals stability differences in ligand-bound multiprotein complexes. *Chem. Biol.* **16,** 382–390 (2009).

56. Hopper, J. T. S. & Oldham, N. J. Collision induced unfolding of protein ions in the gas phase studied by ion mobility-mass spectrometry: The effect of ligand binding on conformational stability. *J. Am. Soc. Mass Spectrom.* **20,** 1851–1858 (2009).
57. Smith, D. P., Radford, S. E. & Ashcroft, A. E. Elongated oligomers in β2-microglobulin amyloid assembly revealed by ion mobility spectrometry-mass spectrometry. *Proc. Natl Acad. Sci. USA* **107,** 6794–6798 (2010).
58. Beveridge, R., Chappuis, Q., MacPhee, C. & Barran, P. Mass spectrometry methods for intrinsically disordered proteins. *Analyst* **138,** 32–42 (2013).
59. Uetrecht, C. *et al.* Stability and shape of hepatitis B virus capsids *in vacuo*. *Angew. Chem. Int. Ed.* **47,** 6247–6251 (2008).
60. Ruotolo, B. T. *et al.* Evidence for macromolecular protein rings in the absence of bulk water. *Science* **310,** 1658–1661 (2005).
61. Jurneczko, E., Kalapothakis, J., Campuzano, I. D. G., Morris, M. & Barran, P. E. Effects of drift gas on collision cross sections of a protein standard in linear drift tube and traveling wave ion mobility mass spectrometry. *Anal. Chem.* **84,** 8524–8531 (2012).
62. Wyttenbach, T., von Helden, G. & Bowers, M. T. Gas-phase conformation of biological molecules: Bradykinin. *J. Am. Chem. Soc.* **118,** 8355–8364 (1996).
63. Baumketner, A. *et al.* Amyloid β-protein monomer structure: A computational and experimental study. *Protein Sci.* **15,** 420–428 (2006).
64. Dear, G. J. *et al.* Sites of metabolic substitution: Investigating metabolite structures utilising ion mobility and molecular modelling. *Rapid Commun. Mass Spectrom.* **24,** 3157–3162 (2010).
65. Cuyckens, F. *et al.* Product ion mobility as a promising tool for assignment of positional isomers of drug metabolites. *Rapid Commun. Mass Spectrom.* **25,** 3497–3503 (2011).
66. Wyttenbach, T., von Helden, G., Batka, J. J., Carlat, D. & Bowers, M. T. Effect of the long-range potential on ion mobility measurements. *J. Am. Soc. Mass Spectrom.* **8,** 275–282 (1997).
67. Shvartsburg, A. A. & Jarrold, M. F. An exact hard-spheres scattering model for the mobilities of polyatomic ions. *Chem. Phys. Lett.* **261,** 86–91 (1996).
68. Shvartsburg, A. A., Schatz, G. C. & Jarrold, M. F. Mobilities of carbon cluster ions: Critical importance of the molecular attractive potential. *J. Chem. Phys.* **108,** 2416–2423 (1998).
69. Jurneczko, E. & Barran, P. E. How useful is ion mobility mass spectrometry for structural biology? The relationship between protein crystal structures and their collision cross sections in the gas phase. *Analyst* **136,** 20–28 (2011).
70. Bleiholder, C., Wyttenbach, T. & Bowers, M. T. A novel projection approximation algorithm for the fast and accurate computation of molecular collision cross sections (I). Method. *Int. J. Mass Spectrom.* **308,** 1–10 (2011).
71. Bleiholder, C., Contreras, S., Do, T. D. & Bowers, M. T. A novel projection approximation algorithm for the fast and accurate computation of molecular collision cross sections (II). Model parameterization and definitions of empirical shape factors for proteins. *Int. J. Mass Spectrom.* **345–347,** 89–96 (2013).
72. Bleiholder, C., Contreras, S. & Bowers, M. T. A novel projection approximation algorithm for the fast and accurate computation of molecular collision cross section (IV). Application to polypeptides. *Int. J. Mass Spectrom.* **354–355,** 275–280 (2013).
73. Wyttenbach, T., Bleiholder, C. & Bowers, M. T. Factors contributing to the collision cross section of polyatomic ions in the kilodalton to gigadalton range: Application to ion mobility measurements. *Anal. Chem.* **85,** 2191–2199 (2013).
74. Hall, Z. & Robinson, C. V. Do charge state signatures guarantee protein conformations? *J. Am. Soc. Mass Spectrom.* **23,** 1161–1168 (2012).
75. Berezovskaya, Y., Porrini, M. & Barran, P. E. The effect of salt on the conformations of three model proteins is revealed by variable temperature ion mobility mass spectrometry. *Int. J. Mass Spectrom.* **345,** 8–18 (2013).
76. Shvartsburg, A. A. & Smith, R. D. Separation of protein conformers by differential ion mobility in hydrogen-rich gases. *Anal. Chem.* **85,** 6967–6973 (2013).
77. Bernstein, S. L. *et al.* Amyloid-β protein oligomerization and the importance of tetramers and dodecamers in the aetiology of Alzheimer's disease. *Nature Chem.* **1,** 326–331 (2009).
78. Grabenauer, M. *et al.* Spermine binding to Parkinson's protein α-synuclein and its disease-related A30P and A53T mutants. *J. Phys. Chem. B* **112,** 11147–11154 (2008).
79. Shimizu, A., Ohe, T. & Chiba, M. A novel method for the determination of the site of glucuronidation by ion mobility spectrometry-mass spectrometry. *Drug Metab. Dispos.* **40,** 1456–1459 (2012).
80. Baker, E. S. *et al.* Diastereomer assignment of an olefin-linked bis-paracyclophane by ion mobility mass spectrometry. *J. Am. Chem. Soc.* **126,** 6255–6257 (2004).
81. Both, P. *et al.* Discrimination of epimeric glycans and glycopeptides using ion-mobility mass spectrometry and its potential for carbohydrate sequencing. *Nature Chem.* **6,** 65–74 (2014).
82. Lee, S. *et al.* Extracted fragment ion mobility distributions: A new method for complex mixture analysis. *Int. J. Mass Spectrom.* **309,** 154–160 (2012).
83. Florance, H. V. *et al.* Evidence for alpha-helices in the gas phase: A case study using melittin from honey bee venom. *Analyst* **136,** 3446–3452 (2011).
84. Jarrold, M. F. Helices and sheets *in vacuo*. *Phys. Chem. Chem. Phys.* **9,** 1659–1671 (2007).
85. Zilch, L. W., Kaleta, D. T., Kohtani, M., Krishnan, R. & Jarrold, M. F. Folding and unfolding of helix-turn-helix motifs in the gas phase. *J. Am. Soc. Mass Spectrom.* **18,** 1239–1248 (2007).
86. McLean, J. R. *et al.* Factors that influence helical preferences for singly charged gas-phase peptide ions: The effects of multiple potential charge-carrying sites. *J. Phys. Chem. B* **114,** 809–816 (2010).
87. Albrieux, F. *et al.* Conformation of polyalanine and polyglycine dications in the gas phase: Insight from ion mobility spectrometry and replica-exchange molecular dynamics. *J. Phys. Chem. A* **114,** 6888–6896 (2010).
88. Albrieux, F. *et al.* Structural preferences of gas-phase M2TMP monomers upon sequence variations. *J. Phys. Chem. A* **115,** 4711–4718 (2011).
89. Wu, C., Klasmeier, J. & Hill, H. H. Atmospheric pressure ion mobility spectrometry of protonated and sodiated peptides. *Rapid Commun. Mass Spectrom.* **13,** 1138–1142 (1999).
90. Liu, D. F. *et al.* Oxytocin-receptor binding: Why divalent metals are essential. *J. Am. Chem. Soc.* **127,** 2024–2025 (2005).
91. Rožman, M. & Gaskell, S. J. Non-covalent interactions of alkali metal cations with singly charged tryptic peptides. *J. Mass Spectrom.* **45,** 1409–1415 (2010).
92. Chen, L., Gao, Y. Q. & Russell, D. H. How alkali metal ion binding alters the conformation preferences of gramicidin A: A molecular dynamics and ion mobility study. *J. Phys. Chem. A* **116,** 689–696 (2012).
93. Garcia, I. R., Giles, K., Bateman, R. H. & Gaskell, S. J. Studies of peptide a- and b-type fragment ions using stable isotope labeling and integrated ion mobility/tandem mass spectrometry. *J. Am. Soc. Mass Spectrom.* **19,** 1781–1787 (2008).
94. Polfer, N. C., Bohrer, B. C., Plasencia, M. D., Paizs, B. & Clemmer, D. E. On the dynamics of fragment isomerization in collision-induced dissociation of peptides. *J. Phys. Chem. A* **112,** 1286–1293 (2008).
95. Saminathan, I. S. *et al.* The extent and effects of peptide sequence scrambling via formation of macrocyclic *b* ions in model proteins. *J. Am. Soc. Mass Spectrom.* **21,** 2085–2094 (2010).
96. Chawner, R., Gaskell, S. J. & Eyers, C. E. Proposal for a common nomenclature for peptide fragment ions generated following sequence scrambling during collision-induced dissociation. *Rapid Commun. Mass Spectrom.* **26,** 205–206 (2012).
97. Moss, C. L. *et al.* Assigning structures to gas-phase peptide cations and cation-radicals. An infrared multiphoton dissociation, ion mobility, electron transfer, and computational study of a histidine peptide ion. *J. Phys. Chem. B* **116,** 3445–3456 (2012).
98. van den Heuvel, R. H. H. & Heck, A. J. R. Native protein mass spectrometry: from intact oligomers to functional machineries. *Curr. Opin. Chem. Biol.* **8,** 519–526 (2004).
99. Kaddis, C. S. & Loo, J. A. Native protein MS and ion mobility: Large flying proteins with ESI. *Anal. Chem.* **79,** 1778–1784 (2007).
100. Heck, A. J. R. Native mass spectrometry: A bridge between interactomics and structural biology. *Nature Methods* **5,** 927–933 (2008).
101. Kondrat, F. D. L., Kowald, G. R., Scarff, C. A., Scrivens, J. H. & Blindauer, C. A. Resolution of a paradox by native mass spectrometry: Facile occupation of all four metal binding sites in the dimeric zinc sensor SmtB. *Chem. Commun.* **49,** 813–815 (2013).
102. Konijnenberg, A., Butterer, A. & Sobott, F. Native ion mobility-mass spectrometry and related methods in structural biology. *BBA-Proteins Proteom.* **1835,** 1239–1256 (2013).
103. Hall, Z., Politis, A., Bush, M. F., Smith, L. J. & Robinson, C. V. Charge-state dependent compaction and dissociation of protein complexes: Insights from ion mobility and molecular dynamics. *J. Am. Chem. Soc.* **134,** 3429–3438 (2012).
104. Raschke, T. M. Water structure and interactions with protein surfaces. *Curr. Opin. Struc. Biol.* **16,** 152–159 (2006).
105. Wolynes, P. G. Biomolecular folding in vacuo!!!(?). *Proc. Natl Acad. Sci. USA* **92,** 2426–2427 (1995).
106. Loo, J. A. *et al.* Electrospray ionization mass spectrometry and ion mobility analysis of the 20S proteasome complex. *J. Am. Soc. Mass Spectrom.* **16,** 998–1008 (2005).
107. Sharon, M. *et al.* 20S proteasomes have the potential to keep substrates in store for continual degradation. *J. Biol. Chem.* **281,** 9569–9575 (2006).
108. Ruotolo, B. T. & Robinson, C. V. Aspects of native proteins are retained in vacuum. *Curr. Opin. Chem. Biol.* **10,** 402–408 (2006).
109. van Duijn, E., Barendregt, A., Synowsky, S., Versluis, C. & Heck, A. J. R. Chaperonin complexes monitored by ion mobility mass spectrometry. *J. Am. Chem. Soc.* **131,** 1452 (2009).
110. Rodriguez-Cruz, S. E., Klassen, J. S. & Williams, E. R. Hydration of gas-phase Gramicidin S $(M + 2H)^{2+}$ ions formed by electrospray: The transition from solution to gas-phase structure. *J. Am. Soc. Mass Spectrom.* **8,** 565–568 (1997).
111. Woenckhaus, J., Hudgins, R. R. & Jarrold, M. F. Hydration of gas-phase proteins: A special hydration site on gas-phase BPTI. *J. Am. Chem. Soc.* **119,** 9586–9587 (1997).

112. Fye, J. L., Woenckhaus, J. & Jarrold, M. F. Hydration of folded and unfolded gas-phase proteins: Saturation of cytochrome c and apomyoglobin. *J. Am. Chem. Soc.* **120,** 1327–1328 (1998).
113. Rodriguez-Cruz, S. E., Klassen, J. S. & Williams, E. R. Hydration of gas-phase ions formed by electrospray ionization. *J. Am. Soc. Mass Spectrom.* **10,** 958–968 (1999).
114. Jarrold, M. F. Peptides and proteins in the vapor phase. *Annu. Rev. Phys. Chem.* **51,** 179–207 (2000).
115. Gao, B., Wyttenbach, T. & Bowers, M. T. Protonated arginine and protonated lysine: Hydration and its effect on the stability of salt-bridge structures. *J. Phys. Chem. B* **113,** 9995–10000 (2009).
116. Kantardjieff, K. A. & Rupp, B. Matthews coefficient probabilities: Improved estimates for unit cell contents of proteins, DNA and protein-nucleic acid complex crystals. *Protein Sci.* **12,** 1865–1871 (2003).
117. Hogan, C. J., Ruotolo, B. T., Robinson, C. V. & de la Mora, J. F. Tandem differential mobility analysis-mass spectrometry reveals partial gas-phase collapse of the GroEL complex. *J. Phys. Chem. B* **115,** 3614–3621 (2011).
118. Breuker, K. & McLafferty, F. W. Stepwise evolution of protein native structure with electrospray into the gas phase, 10^{-12} to 10^{2} s. *Proc. Natl Acad. Sci. USA* **105,** 18145–18152 (2008).
119. Zhao, Q. *et al.* Effects of ion/ion proton transfer reactions on conformation of gas-phase cytochrome c ions. *J. Am. Soc. Mass Spectrom.* **21,** 1208–1217 (2010).
120. Badman, E. R., Myung, S. & Clemmer, D. E. Evidence for unfolding and refolding of gas-phase cytochrome c ions in a Paul trap. *J. Am. Soc. Mass Spectrom.* **16,** 1496–1497 (2005).
121. Wyttenbach, T. & Bowers, M. T. Structural stability from solution to the gas phase: Native solution structure of ubiquitin survives analysis in a solvent-free ion mobility-mass spectrometry environment. *J. Phys. Chem. B* **115,** 12266–12275 (2011).
122. Lorenzi, M. *et al.* Conformational selection underlies recognition of a molybdoenzyme by its dedicated chaperone. *PLoS ONE* **7**, e49523 (2012).
123. Wang, S. C. *et al.* Ion mobility mass spectrometry of two tetrameric membrane protein complexes reveals compact structures and differences in stability and packing. *J. Am. Chem. Soc.* **132,** 15468–15470 (2010).
124. Boryski, A. J. & Robinson, C. V. The 'sticky business' of cleaning gas-phase membrane proteins: A detergent oriented perspective. *Phys. Chem. Chem. Phys.* **14,** 14439–14449 (2012).
125. Leney, A. C., McMorran, L. M., Radford, S. E. & Ashcroft, A. E. Amphipathic polymers enable the study of functional membrane proteins in the gas phase. *Anal. Chem.* **84,** 9841–9847 (2012).
126. Ashcroft, A. E. Mass spectrometry and the amyloid problem - How far can we go in the gas phase? *J. Am. Soc. Mass Spectrom.* **21,** 1087–1096 (2010).
127. Smith, D. P., Woods, L. W., Radford, S. E. & Ashcroft, A. E. Structure and dynamics of oligomeric intermediates in β_2-microglobulin self-assembly. *Biophys. J.* **101,** 1238–1247 (2011).
128. Bernstein, S. L. *et al.* Amyloid β-protein: Monomer structure and early aggregation states of Aβ42 and is Pro^{19} alloform. *J. Am. Chem. Soc.* **127,** 2075–2084 (2005).
129. Gessel, M. M. *et al.* Aβ(39–42) modulates Aβ oligomerization but not fibril formation. *Biochemistry* **51,** 108–117 (2012).
130. Zheng, X. *et al.* Z-Phe-Ala-diazomethylketone (PADK) disrupts and remodels early oligomer states of Alzheimer diseases Aβ42 protein. *J. Biol. Chem.* **287,** 6084–6088 (2012).
131. Amijee, H. *et al.* The N-methylated peptide SEN304 powerfully inhibits Aβ(1–42) toxicity by perturbing oligomer formation. *Biochemistry* **51,** 8338–8352 (2012).
132. Hernandez, H. & Robinson, C. V. Determining the stoichiometry and interactions of macromolecular assemblies from mass spectrometry. *Nature Protoc.* **2,** 715–726 (2007).
133. Zhou, M. *et al.* Mass spectrometry of intact V-type ATPases reveals bound lipids and the effects of nucleotide binding. *Science* **334,** 380–385 (2011).
134. Baker, E. S., Dupuis, N. F. & Bowers, M. T. DNA hairpin, pseudoknot, and cruciform stability in a solvent-free environment. *J. Phys. Chem. B* **113,** 1722–1727 (2009).
135. Chan, Y. T. *et al.* Design, synthesis, and traveling wave ion mobility mass spectrometry characterization of iron(II)- and ruthenium(II)-terpyridine metallomacrocycles. *J. Am. Chem. Soc.* **133,** 11967–11976 (2011).
136. Larriba, C. & de la Mora, J. F. The gas phase structure of coulombically stretched polyethylene glycol ions. *J. Phys. Chem. B* **116,** 593–598 (2012).
137. Arcella, A. *et al.* Structure of triplex DNA in the gas phase. *J. Am. Chem. Soc.* **134,** 6596–6606 (2012).
138. Nagesh, N. & Chatterji, D. Ammonium ion at low concentration stabilizes the G-quadruplex formation by telomeric sequence. J. *Biochem. Bioph. Meth.* **30,** 1–8 (1995).
139. Baker, E.S., Bernstein, S.L., Gabelica, V., De Pauw, E. & Bowers, M.T. G-quadruplexes in telomeric repeats are conserved in a solvent-free environment. *Int. J. Mass Spectrom.* **253,** 225–237 (2006).
140. Rosu, F., Gabelica, V., Poncelet, H. & De Pauw, E. Tetramolecular G-quadruplex formation pathways studied by electrospray mass spectrometry. *Nucleic Acids Res.* **38,** 5217–5225 (2010).
141. Wyttenbach, T., von Helden, G. & Bowers, M. T. Conformations of alkali ion cationized polyethers in the gas phase: Polyethylene glycol and bis[(benzo-15-crown-5)-15-ylmethyl] pimelate. *Int. J. Mass Spectrom. Ion Processes* **165–166,** 377–390 (1997).
142. von Helden, G., Wyttenbach, T. & Bowers, M. T. Conformation of macromolecules in the gas phase: Use of matrix-assisted laser desorption methods in ion chromatography. *Science* **267,** 1483–1485 (1995).
143. De Winter, J. *et al.* Size dependence of the folding of multiply charged sodium cationized polylactides revealed by ion mobility mass spectrometry and molecular modelling. *Chem. Eur. J.* **17,** 9738–9745 (2011).
144. Alsharaeh, E. H. & El-Shall, M. S. Ion mobility study of the mechanism of the gas phase thermal polymerization of styrene and the structures of the early oligomers. *Polymer* **52,** 5551–5559 (2011).
145. Ujma, J. *et al.* Shapes of supramolecular cages by ion mobility mass spectrometry. *Chem. Commun.* **48,** 4423–4425 (2012).
146. Brocker, E. R., Anderson, S. E., Northrop, B. H., Stang, P. J. & Bowers, M. T. Structures of metallosupramolecular coordination assemblies can be obtained by ion mobility spectrometry-mass spectrometry. *J. Am. Chem. Soc.* **132,** 13486–13494 (2010).
147. Lalli, P. M. *et al.* Resolution of isomeric multi-ruthenated porphyrins by travelling wave ion mobility mass spectrometry. *Rapid Commun. Mass Spectrom.* **26,** 263–268 (2012).
148. Li, X. *et al.* Separation and characterization of metallosupramolecular libraries by ion mobility mass spectrometry. *Anal. Chem.* **83,** 6667–6674 (2011).
149. Zhong, Y., Hyung, S.-J. & Ruotolo, B. T. Characterizing the resolution and accuracy of a second-generation traveling-wave ion mobility separator for biomolecular ions. *Analyst* **136,** 3534–3541 (2011).
150. Li, H., Bendiak, B., Siems, W. F., Gang, D. R. & Hill, H. H. Jr. Carbohydrate structure characterisation by tandem ion mobility mass spectrometry $(IMMS)^2$. *Anal. Chem.* **85,** 2760–2769 (2013).
151. Baker, E. S. *et al.* Ion mobility spectrometry-mass spectrometry performance using electrodynamic ion funnels and elevated drift gas pressures. *J. Am. Soc. Mass Spectrom.* **18,** 1176–1187 (2007).
152. Giles, K., Williams, J. P. & Campuzano, I. Enhancements in travelling wave ion mobility resolution. *Rapid Commun. Mass Spectrom.* **25,** 1559–1566 (2011).
153. Merenbloom, S. I., Glaskin, R. S., Henson, Z. B. & Clemmer, D. E. High-resolution ion cyclotron mobility spectrometry. *Anal. Chem.* **81,** 1482–1487 (2009).
154. Glaskin, R. S., Valentine, S. J. & Clemmer, D. E. A scanning frequency mode for ion cyclotron mobility spectrometry. *Anal. Chem.* **82,** 8266–8271 (2010).
155. Glaskin, R. S., Ewing, M. A. & Clemmer, D. E. Ion trapping for ion mobility spectrometry measurements in a cyclical drift tube. *Anal. Chem.* **85,** 7003–7008 (2013).
156. Shaffer, S. A. *et al.* A novel ion funnel for focusing ions at elevated pressure using electrospray ionization mass spectrometry. *Rapid Commun. Mass Spectrom.* **11,** 1813–1817 (1997).
157. Kemper, P. R., Dupuis, N. F. & Bowers, M. T. A new, higher resolution, ion mobility mass spectrometer. *Int. J. Mass Spectrom.* **287,** 46–57 (2009).
158. Ranjbar, B. & Gill, P. Circular dichroism techniques: Biomolecular and nanostructural analyses - A review. *Chem. Biol. Drug Des.* **74,** 101–120 (2009).
159. Roberts, G. & Lian, L. Y. *Protein NMR Spectroscopy: Practical Techniques and Applications* (Wiley, 2011).
160. Murray, K. K. *et al.* Definitions of terms relating to mass spectrometry (IUPAC recommendations 2013). *Pure Appl. Chem.* **85,** 1515–1609 (2013).

Acknowledgements

We acknowledge the financial support of the Biotechnology and Biological Sciences Research Council (BB/H007113/1, BB/G009058/1, BB/F00561X/1) and the European Commission's Seventh Framework Programme (FP7), which funded GlycoBioM. C.G. is supported by a BBSRC doctoral training grant. Finally, we thank P. Eyers for a critical reading of the review.

Author contributions

F.L., S.W.H. and C.J.G. contributed equally to this paper.

Additional information

Reprints and permissions information is available online at www.nature.com/reprints. Correspondence and requests for materials should be addressed to C.E.E.

Competing financial interests

The authors declare no competing financial interests.